

1 **Seismic swarm preceding the 2017 Mount Agung eruption in Bali**
2 **(Indonesia) enhanced by the matched filter approach**

3 Dimas Sianipar^{1,2}, Emi Ulfiana^{1,3}, Renhard Sipayung^{1,4}

4 ¹Badan Meteorologi, Klimatologi, dan Geofisika (BMKG), Jakarta 10720, Indonesia

5 ²Sekolah Tinggi Meteorologi, Klimatologi, dan Geofisika (STMKG), Tangerang Selatan,
6 Banten, 15221, Indonesia

7 ³BMKG Stasiun Geofisika Sanglah, Denpasar, Bali, Indonesia

8 ⁴BMKG Stasiun Geofisika Banjarnegara, Jawa Tengah, Indonesia

9 **Corresponding author:** Dimas Sianipar (<https://orcid.org/0000-0002-9895-4616>)

10

11 This manuscript has been submitted for publication and is currently undergoing peer review.
12 Subsequent versions of this manuscript may have slightly different content. If accepted, the
13 final versions of this manuscript will be available via the “Peer-reviewed Publication DOI”
14 link on the EarthArXiv webpage. Please check for the newest version before referencing this
15 preprint.

16

17 Please feel free to contact any of the authors; we welcome constructive feedback.

18

19

20

21 **Seismic swarm preceding the 2017 Mount Agung eruption in Bali**
22 **(Indonesia) enhanced by the matched filter approach**

23 Dimas Sianipar^{1,2}, Emi Ulfiana^{1,3}, Renhard Sipayung^{1,4}

24 ¹Badan Meteorologi, Klimatologi, dan Geofisika (BMKG), Jakarta 10720, Indonesia

25 ²Sekolah Tinggi Meteorologi, Klimatologi, dan Geofisika (STMKG), Tangerang Selatan,
26 Banten, 15221, Indonesia

27 ³BMKG Stasiun Geofisika Sanglah, Denpasar, Bali, Indonesia

28 ⁴BMKG Stasiun Geofisika Banjarnegara, Jawa Tengah, Indonesia

29 **Corresponding author:** Dimas Sianipar (<https://orcid.org/0000-0002-9895-4616>)

30 **Email:** dsj.sianipar@stmkg.ac.id, dimas.salomo@bmgk.go.id

31

32 **Key Points:**

- 33 • Reappraisal of the seismic swarm preceding the 2017 Mount Agung eruption by
34 waveform-based relocation and matched filter technique.
- 35 • We detect fourteen times more events (5,803 earthquakes) than the routine earthquake
36 catalog (407 earthquakes).
- 37 • We show the updated spatiotemporal evolution of the swarm seismicity before the
38 eruption.

39

40

41 **Abstract**

42 Intense swarm seismicity took place before the 2017 Mount Agung eruption in Bali
43 (Indonesia). However, the earthquake sequences were not well seismological documented.
44 Besides, there was a substantial delay between the peak of the seismic activity (late
45 September) and the onset of the impending eruption (late November). Here, we apply
46 waveform-based hypocenter relocation and matched filter technique (MFT) to enhance the
47 earthquake catalog of the swarm that associated with the eruption. We detect fourteen times
48 more events (5,803) than the routine catalog (407) from 1 August 2017 to 1 December 2017.
49 The intense swarm initiated on 20 September 2017 at ~09:00 UTC and the peak of the swarm
50 occurred during 22-24 September with 1,473 events. The updated spatiotemporal evolution of
51 the swarm seismicity shed light on the processes involved in a reawaking of a volcano and
52 highlighted the use of MFT in volcanoes monitoring using the existing regional seismic
53 network.

54

55 **Plain Language Summary**

56 The sequence of earthquake swarms before the Mount Agung eruption in 2017 was not well
57 investigated due to the lack of local seismic observations close to the summit. We overcome
58 this limitation by applying advanced seismic relocation and detection using an existing
59 regional seismic network that routinely used for ‘tectonic’ earthquake monitoring in
60 Indonesia. The detection approach benefits from waveform cross-correlations between the
61 digital continuous seismograms and template seismograms. We detect and locate fourteen
62 times more earthquakes than that of had been cataloged by regular earthquake monitoring in
63 Bali, Indonesia. The more robust and improved swarm catalog provides information about
64 processes during the volcanic unrest of Mount Agung before the impending eruptions.

65 **Index Terms:**

66 7280 Volcano Seismology (4302, 8419)

67 8419 Volcano Monitoring (4302, 7280)

68 7215 Earthquake source observations (1240)

69 7294 Seismic Instruments and Networks (0935, 3025)

70

71 **Keywords:** Mount Agung, Matched filter, Swarm, Volcano-tectonic (VT)

72

73 **1 Introduction**

74 Mount Agung is a ~3000-m high stratovolcano that dominated the northeastern zone
75 of Bali Island in Indonesia (Figure 1). After having been inactive for about half a century, in
76 late November 2017, Mount Agung erupted for the first time since 1963-64. The previous
77 study indicated a frequency of one explosive eruption ($VEI \geq 2-3$) per century (on average) for
78 Mount Agung, and in its ~5000-year record, marked by periods of background eruptive rates
79 identical to general subduction zone volcanoes then changed to durations of increased
80 eruptive rates (Fontijn *et al.*, 2015). It attributed to increased magma supply rates from the
81 depth that suggesting frequent open-system processes of magmatic differentiation. Repeated
82 intrusions of basaltic magmas into basaltic andesitic to andesitic reservoirs obtained its
83 erupted magmas (Fontijn *et al.*, 2015).

84 The timeline during the 2017 volcanic crisis of Mount Agung has been described in
85 the previous studies (e.g., Albino *et al.*, 2019; Syahbana *et al.*, 2019). The first
86 phreatomagmatic eruption occurred on 21 November and the onset of the magmatic eruption

87 occurred on 25 November (Syahbana *et al.*, 2019). These eruptions were preceded by a series
88 of energetic seismic swarms (Figure 1). However, these earthquakes were not well cataloged.
89 It remains unclear about the source origin of this swarm and its spatiotemporal evolution as
90 well as its association with the impending eruption. The lack of information about this swarm
91 was due to the lack of capability in detecting small earthquakes by the routine methodology
92 applied in regular monitoring. Moreover, the 2017 seismic swarm occurred without
93 immediate eruption; the eruption began about several weeks after the seismicity had already
94 decreased. Robust information about precursory seismic swarm during a volcanic crisis is
95 important for proper response and eruption forecasting.

96 In this study, we perform a matched filter technique (MFT; or template matching) to
97 identify small, uncataloged earthquakes based on their similarity to target events (i.e.,
98 templates). We provide a more complete and improved catalog of the swarm seismicity and
99 then summarize the 2017 unrest at Mount Agung by showing the updated spatiotemporal
100 evolution of the swarm based on the MFT catalog. We highlight the application of MFT in
101 monitoring volcanic swarm using the existing regional broadband seismic network.

102

103 **2 Matched Filter Technique (MFT)**

104 Based on the national catalog of Badan Meteorologi, Klimatologi, dan Geofisika
105 (BMKG), the seismicity near Mount Agung from September to November 2017 located
106 mostly NW of Mount Agung (Figure S1, S2). Some 407 events had been identified by
107 BMKG with magnitude ranging from 2.2 to 4.9 and depth between 5 and 20 km (Figure 1a,
108 b). The magnitude of completeness (M_c) of this catalog is 2.7 (local magnitude, Figure S3).
109 The seismicity contains many smaller earthquakes compared with larger events thus yielded a
110 relatively large b-value of frequency-magnitude distribution (FMD), i.e., $b= 1.3$ (Figure 1d,

111 S3). In this study, we use all of these 407 events as our template candidates for MFT. The
112 MFT has been applied in other volcanic areas, for instance, at Mount Ontake, Japan (Kato *et*
113 *al.*, 2015), and Piton De La Fournaise volcano (Duputel *et al.*, 2019).

114 We collected the seismic data for all of these earthquakes and use them as templates
115 candidates in our scanning through the continuous waveforms for potential detectable
116 earthquakes associated with the 2017 eruption. We selected data from six regional broadband
117 three-component stations (i.e., 18 channels) with a distance less than 170 km from the
118 summit and with good azimuthal coverage.

119 We consider all of the earthquakes here are the type of volcano-tectonic (VT)
120 earthquakes showing by its high-frequency contents (Figure S4-S7) and characterized by
121 clear arrivals of P- and S-waves on their seismograms (Figure 2) and their adjoining locations
122 with the volcanoes (McNutt, 2005; White and McCausland, 2016). However, we observe
123 obvious S-wave shadow at station SRBI and DNP (Figure 2, S8) and we will discuss this
124 topic in the discussion section.

125 We pick the P- and S-wave arrival times for the 407 events and enhance the quality of
126 locations by applying double-difference relocation improved with waveform cross-correlation
127 data (Waldhauser and Ellsworth, 2000, see Text S1). The result of the relocation indicates
128 most of the events located between Mount Agung and Batur Caldera, but closer to Mount
129 Abang (Figure 2). There is also one obvious separated cluster in the NE of Mount Agung
130 (Figure 3).

131 The MFT procedure here generally follows that of Meng *et al.* (2013; 2018). We use
132 continuous waveforms containing each 24-hours seismogram for a period of 1 August to 1
133 December 2017 (i.e., 123 days). We use SH* channels data with a sampling rate of 40 Hz.
134 Two-way pass, fourth-order, Butterworth band-pass filter with a corner frequency of 1 and 15

135 Hz was applied to both continuous and template waveforms. Among 407 template candidates,
136 we select quality seismograms of 257 templates that have been satisfactorily relocated and
137 having signal-to-noise ratio (SNR) >5 recorded by at least 8 channels of seismograms (≥ 3
138 stations).

139 The template waveform comprises signals within a time window of 8 s starting from
140 0.5 s before the picked P-wave arrival time for the vertical component and 0.5 s before the
141 picked S-wave arrival time for the two horizontal components. We compute the correlation-
142 coefficient (CC) between the template and continuous waveform by using a correlating time
143 step of 0.025 s; i.e., the computing window moves forward by one data point. We compute
144 the mean CC among all components at each time point allowing one data point shift (Meng *et*
145 *al.*, 2013). A perfect self detection should have a mean CC of 1, i.e., the template waveforms
146 should perfectly detect itself in the continuous waveforms. The newly positive detection
147 threshold is set to be the sum of the median value and 15 times the median absolute deviation
148 (MAD) of the mean CC trace. The location of the detected event is assigned to be the same
149 with that of the corresponding template with the highest mean CC within 2 s, assuming that
150 the template and new detected event are collocated based on their high correlation. The
151 magnitude of the detected event is computed based on the peak amplitude ratios between the
152 detected and template event (Meng *et al.*, 2013). An example of MFT detection is provided in
153 Figure 4 and S9.

154

155 **3 Results**

156 By using a relatively high threshold, we detect 5,803 events including 257 perfect self
157 detections with mean CC= 1 (Figure 5). This is equivalent to about fourteen times the number
158 of events reported by BMKG. Completeness of the MFT catalog is 2.4 (local magnitude);

159 lower than 2.7 of the BMKG catalog (Figure S3). The magnitude ranges from 1.5 to 4.9 and
160 20 events have magnitude >3.5 (Figure 5d); one of them is newly detected i.e., the 2017-10-
161 18 00:24 UTC with magnitude 3.6. As expected, because MFT detects smaller magnitudes,
162 the b-value for the entire seismicity increases became $b= 1.6$.

163 Some new detections have a large correlation with the detecting templates, for
164 example, a magnitude 3.1 (Figure S9, Table S2) is newly detected with mean CC of 0.946 on
165 21 September 09:07:17 UTC by template 20170921104359 ($M=3.3$; 12 channels with SNR $>$
166 5). Another example is a magnitude 3.1 on 13 October 15:32 UTC detected with mean CC of
167 0.857 by a magnitude 3.6 template (Figure 4).

168 We detect only two small events that occurred in the first 50 days (from 1 August to
169 19 September) with magnitude 2.7 and 2.6 (15 August), respectively (Figure S10, S11).
170 Intense seismicity was firstly initiated on 20 September at 09:00 UTC with a small event at
171 depth ~ 9.7 km and located closer to Mount Agung (Figure 5). We detect 85 events during the
172 day of 20 September as compared to only two events in the BMKG catalog. The seismicity
173 rapidly accelerated and more than 300 events per day are detected during 21-26 September
174 while the peak of the swarm occurred during 22-24 September (UTC) with 1,473 detected
175 events (commenced by the first green line on Figure 5a).

176 The seismicity during 20-22 September mostly occurred at ~ 9 to 11 km depths,
177 however, during the early peak period with the rapid acceleration of seismicity (started on 22
178 September), the earthquakes were located at deeper locations up to ~ 13 km in the mid-crust
179 (Figure 5b). The rate of seismicity also slightly increase on 26 and 27 September due to the
180 existence of two $M>4$ events (black stars in Figure 5a). We observe three obvious peaks of
181 the number of seismicity on 23 September, 6 October, and 18 October 2017, respectively that
182 marked three occasions of distinct increases in the rate of VT earthquakes (Figure 5a). The

183 increase of seismicity in the mid of October 2017 was also accompanied by some deeper
184 events.

185 Seismicity completely decreased on 20-21 October (< 20 events per day, marked by
186 the second green line on Figure 5a). In total, the duration of intensive swarm (e.g., with > 6
187 detected events per day) was 39 days, i.e., 20 September to 28 October. After about 10 days
188 of quiescence (e.g., ≤ 6 events per day), the seismicity rate slightly increase on 8 November
189 due to an M4.9 earthquake (marked by the third green line on Figure 5a) and its early
190 aftershocks. However, these earthquakes appeared in a different location, i.e., in NE of
191 Mount Agung.

192

193 **4 Discussions and Conclusion**

194 In this study, we perform hypocenter relocation and MFT to enhance the detection of
195 lower magnitude VT events before the 2017 Mount Agung eruption. MFT employs many
196 template waveforms and identifies small events through waveform cross-correlation (Meng *et*
197 *al.*, 2018). Zhang and Wen (2015) and Kato *et al.* (2015) also utilized a similar technique to
198 swarm seismicity preceding eruptions of Mount Ontake in Japan.

199 We select six broadband regional stations to investigate the swarm associated with the
200 eruption (Figure 1, 4). To ensure the quality of detection, we use a high threshold (Meng *et*
201 *al.*, 2013). Using a lower threshold (e.g., 6-14 x MAD as applied in some references) would
202 result in false detections. We decreased the completeness of the swarm catalog from 2.7 to
203 2.4 and the FMD is better fitted as cumulative normal distribution than that of the BMKG
204 catalog (Figure S3). Mount Agung has swarm seismicity with the maximum peak in the

205 opening of the sequence. Seismicity continued to accelerate rapidly toward its peak in just
206 one day after the detectable initiation.

207 Our waveform-based hypocenter relocation indicates that all events took place at
208 depth of 6.8 to 13.1 km (mostly at 9 to 13 km) or in the mid-crust (Figure 3, S12). It is
209 noteworthy that Geiger *et al.* (2018) proposed two major magma storage regions of Mount
210 Agung located at 18 to 22 km depth (near the Moho discontinuity) and 3 to 7 km depth. In
211 other words, the seismicity located midway between the deeper and shallower magma storage
212 zone.

213 Besides, hypocenters of the swarm can also be divided into two groups. The first
214 group is the denser-seismicity beneath Mount Agung and Batur Caldera (Figure 3d). Most of
215 the refined seismicity during the peak of the swarm located in this group and persistently took
216 place at ~9-11 km depth with only two occurrences at the deeper location (up to 13 km
217 depth), i.e., when the peak seismicity occurred (22 September) and on mid-October. The
218 episode of earthquakes at deeper locations in a short period during 22 September is
219 interesting. This might pronounce the ‘strong’ initiation of a dike intrusion. VT seismicity
220 was considered to reflect the stresses induced by the dike propagation (e.g., Roman and
221 Cashman, 2006).

222 Another group is a cluster of M4.9 sequence that contains the M4.9 and its
223 aftershocks located ~8-10 km NE of Mount Agung. Their epicenters formed a NE-SW
224 lineament (Figure 2) and the hypocenters formed a presence of a dipping structure (Figure 3).
225 We interpret this cluster as seismicity occurred at a local tectonic fault. The seismicity in this
226 cluster was recorded in station DNP (SW of epicenters) with no obvious S-wave (or so-called
227 ‘S-wave shadow’, Figure S8) because the propagation of seismic rays might go through the
228 magma plumbing zone of Mount Agung. It is noteworthy that S-wave cannot travel through

229 liquids. This also marks a potentially seismic detection of a magma reservoir beneath Mount
230 Agung by S-wave shadow (e.g., Lin *et al.*, 2018). In contrast, the S-wave of the M4.2 event
231 (26 September) from the first cluster is clear at station DNP but hardly observed at station
232 SRBI (NW of the epicenter) as shown in Figure 2. This might be due to the existence of
233 magma beneath either Mount Abang and Batur Caldera.

234 After the onset of the M4.9 event, Pusat Vulkanologi dan Mitigasi Bencana Geologi
235 (PVMBG) of Indonesia reported the emergence of low-frequency (LF) events and volcanic
236 tremors beneath Mount Agung (Figure 5). However, the proximal shallow seismic activity
237 that directly associated with the impending eruption might be very small (e.g., $M < 2.4$) thus
238 could not be detected by the regional network through our MFT detection and its progression
239 toward the summit might be only detected by very close seismic stations.

240 Syahbana *et al.* (2019) reported that the intense swarm had been initiated on 16
241 September as shown by the increase of Real-time Seismic Amplitude Measurement (RSAM)
242 at a local short-period station (Figure 5c). However, in this study, MFT detection by using a
243 regional network indicates that the swarm was initiated on 20 September ~09:00 UTC. This
244 discrepancy might indicate that the seismic events that occurred from 16 to 19 September
245 were smaller than 2.4, above which our MFT catalog can be considered reasonably complete,
246 thus could not be detected by the regional stations. In general, the pattern of seismicity rate
247 changes determined by MFT detection (Figure 5a) is similar to the RSAM graph from the
248 local short-period station (Figure 5c). The swarm accelerated on 22 September 2017 as also
249 shown by the seismic record at a local station (RSAM values peaked on 22 September in
250 station TMKS).

251 Syahbana *et al.* (2019) inferred that magma intruded into the mid-crust in early 2017
252 and in August 2017, in advance of the intrusion of a dike between Mount Agung and Abang

253 that initiated swarm seismicity in late September. The record of the N component of REND
254 (GNSS) indicated ~20 cm southward movement (Figure 5c) from August to late September,
255 away from Mount Agung. Syahbana *et al.* (2019) interpreted this displacement as a sign of
256 deep inflation beneath Mount Agung. This deep inflation was aseismic, confirmed by the
257 RSAM of TMKS station and the MFT detection in this study (Figure 5). The intense swarm
258 activity was initiated near the end of this deep inflation. During the period of 16 to 23
259 September, the REND displacement was changing become northward movement. Syahbana
260 *et al.* (2019) interpreted this northward movement (toward Mount Agung) as the sign of deep
261 deflation.

262 By using InSAR analysis and 3D numerical models, Albino *et al.* (2019) indicated the
263 2017 seismic swarm was related to the intrusion of a deep, sub-vertical magmatic dike
264 between Agung and Batur. Their inferred dike is plotted in Figure 3. Our swarm seismicity in
265 this study is generally consistent with the location of the dike proposed by them (Figure 3).
266 We agree about the existence of a vertically and laterally interconnected system undergoing
267 recurring magma mixing beneath Mount Agung and Batur. Based on the work of Albino *et*
268 *al.* (2019), a scheme of transport from a deep mafic source to a shallow andesitic reservoir is
269 consistent with the geometry of the 2017 dike, while it was controlled by stresses from the
270 topographic load. Besides, the corrected InSAR time series indicates a broad pre-eruptive
271 uplift (Figure 5b) between Mount Agung and Batur (Point 'A', Figure 2) primarily during 6
272 to 14 October or about two weeks after the initiation of the swarm and one month before the
273 eruption (Albino *et al.*, 2020). This uplift corresponds to the general decreases in the rate of
274 VT earthquakes with one of the little peaks of the seismicity shown in Figure 5.

275 In summary, volcanic unrest and eruption at Agung provide important lessons for
276 eruption forecasting (Gertisser *et al.*, 2018). The intensive period of the VT swarm occurred
277 from 20 September to 28 October (39 days) while the peak of seismicity occurred from 22 to

278 24 September (UTC). We identify two clusters of seismicity, i.e., in NW of Mount Agung
279 (i.e., magmatic dike) and NE of Mount Agung (i.e., tectonic fault structure). As noted by
280 Syahbana *et al.* (2019), uncertainties in forecasting the eruption were subjectively situated
281 due to lack of deformation data and limitations of seismic data. Here, we attempted to
282 provide an advanced complementary way to overcome the limitation of small earthquake
283 detection using an existing regional network. However, we also could not detect the proximal
284 shallow seismicity that occurred just before the eruption. Moreover, the updated
285 spatiotemporal evolution and cumulative seismic moment of VT events (Figure S12)
286 provided by MFT detection here could help in estimating the ongoing situation beneath
287 Mount Agung (e.g., White and McCausland, 2016).

288 The potential trigger mechanism for a ‘late’ eruption at a stratovolcano is essentially
289 challenging to assess; in this case, it might be the deep intrusion of magma, dike-induced
290 swarm, or the tectonic triggering from the M4.9 event. Because seismicity initially declined
291 after the 39-days dike-induced swarm and the low-frequency (LF) and volcanic tremor events
292 shortly took place after the M4.9, we tend to select the mechanism of that M4.9 could
293 catalyze the eruption by either the permanent displacement (static triggering) or propagation
294 of seismic waves (dynamic triggering) (e.g., McNutt, 2005; Walter *et al.*, 2007).
295 Understanding every signal that came from beneath Mount Agung is important for volcanic
296 hazard for the people of Bali and beyond. It is noteworthy that the 1963-64 Mount Agung
297 eruption yielded serious fatalities with almost 1,500 people killed by its pyroclastic flows and
298 fast-flowing volcanic mudflows (lahars). Our results show improvements in the earthquake
299 catalog of the seismic swarm that feasibly applied shortly for monitoring of Mount Agung
300 using existing regional networks.

301

302 **Acknowledgements**

303 Earthquake catalog can be downloaded from BMKG repository
304 (http://repogempa.bmkg.go.id/repo_new/repository.php) and is available in Table S1 and S2.
305 Dataset for hypocenter relocation and MFT used in this study can be accessed from Zenodo
306 (<https://doi.org/10.5281/zenodo.3820934>). We are thankful to Xiaofeng Meng and Zhigang
307 Peng for the matched filter code. We also thank PVMBG of Indonesia for continuous efforts
308 in the monitoring of Mount Agung. The manuscript benefits from earthquakes information by
309 Daryono (BMKG). Constructive comments from Fabien Albino to the early draft of this
310 manuscript are greatly appreciated. All figures are created by using Generic Mapping Tools
311 (GMT) (Wessel *et al.*, 2013).

312

313 **References**

- 314 Albino, F., J. Biggs, C. Yu, and Z. Li (2020), Automated methods for detecting volcanic
315 deformation using Sentinel-1 InSAR time series illustrated by the 2017–2018 unrest at
316 Agung, Indonesia, *Journal of Geophysical Research: Solid Earth*, 125,
317 e2019JB017908. <https://doi.org/10.1029/2019JB017908>
- 318 Albino, F., J. Biggs, and D.K. Syahbana (2019), Dyke intrusion between neighbouring arc
319 volcanoes responsible for 2017 pre-eruptive seismic swarm at Agung, *Nat Commun*,
320 10(1), 748. <https://doi.org/10.1038/s41467-019-08564-9>.
- 321 Duputel, Z., O. Lengliné, and V. Ferrazzini (2019), Constraining Spatiotemporal
322 Characteristics of Magma Migration at Piton De La Fournaise Volcano From Pre-
323 eruptive Seismicity, *Geophysical Research Letters*, 46(1), pp.119-127.

- 324 Fontijn, K., F. Costa, I. Sutawidjaja, C.G. Newhall, and J.S. Herrin (2015), A 5000-year
325 record of multiple highly explosive mafic eruptions from Gunung Agung (Bali,
326 Indonesia): implications for eruption frequency and volcanic hazards, *Bulletin of*
327 *Volcanology*, 77(7), p.59.
- 328 Geiger, H., V.R. Troll, E.M. Jolis, F.M. Deegan, C. Harris, D.R. Hilton, and C. Freda (2018),
329 Multi-level magma plumbing at Agung and Batur volcanoes increases risk of hazardous
330 eruptions, *Scientific Reports*, 8(1), pp.1-14.
- 331 Gertisser, R., F.M. Deegan, V.R. Troll, and K. Preece (2018), When the gods are angry:
332 volcanic crisis and eruption at Bali's great volcano, *Geology Today*, 34(2), pp.62-65.
- 333 Kato, A., T. Terakawa, Y. Yamanaka, Y. Maeda, S. Horikawa, K. Matsuhiro, and T. Okuda
334 (2015), Preparatory and precursory processes leading up to the 2014 phreatic eruption
335 of Mount Ontake, Japan, *Earth, Planets and Space*, 67(1), pp.1-11.
- 336 Lin, C.H., Y.C. Lai, M.H. Shih, H.C. Pu, and S.J. Lee (2018), Seismic Detection of a Magma
337 Reservoir beneath Turtle Island of Taiwan by S-Wave Shadows and Reflections,
338 *Scientific Reports*, 8(1), pp.1-12.
- 339 McNutt, S.R. (2005), Volcanic seismology, *Annu. Rev. Earth Planet. Sci.*, 32, pp.461-491.
- 340 Meng, X., H. Yang, and Z. Peng (2018), Foreshocks, b value map, and aftershock triggering
341 for the 2011 Mw 5.7 Virginia Earthquake, *Journal of Geophysical Research: Solid*
342 *Earth*, 123(6), pp.5082-5098.
- 343 Meng, X., Z. Peng, and J.L. Hardebeck (2013), Seismicity around Parkfield correlates with
344 static shear stress changes following the 2003 Mw6.5 San Simeon earthquake, *Journal*
345 *of Geophysical Research: Solid Earth*, 118(7), pp.3576-3591.

- 346 Roman, D.C. and K.V. Cashman (2006), The origin of volcano-tectonic earthquake swarms,
347 *Geology*, 34(6), pp.457-460.
- 348 Syahbana, D.K., K. Kasbani, G. Suantika, O. Prambada, A.S. Andreas, U.B. Saing, S.L.
349 Kunrat, S. Andreastuti, M. Martanto, E. Kriswati, and Y. Suparman (2019), The 2017–
350 19 activity at Mount Agung in Bali (Indonesia): Intense unrest, monitoring, crisis
351 response, evacuation, and eruption, *Scientific Reports*, 9(1), pp.1-17.
- 352 Waldhauser, F. and W.L. Ellsworth (2000), A double-difference earthquake location
353 algorithm: Method and application to the northern Hayward fault, California, *Bulletin of*
354 *the Seismological Society of America*, 90(6), pp.1353-1368.
- 355 Walter, T.R., R. Wang, M. Zimmer, H. Grosser, B. Lühr, and A. Ratdomopurbo (2007),
356 Volcanic activity influenced by tectonic earthquakes: static and dynamic stress
357 triggering at Mt. Merapi, *Geophysical Research Letters*, 34(5).
- 358 Wessel, P., W.H. Smith, R. Scharroo, J. Luis, and F. Wobbe (2013), Generic mapping tools:
359 improved version released, *Eos, Transactions American Geophysical Union*, 94(45),
360 pp.409-410.
- 361 White, R. and W. McCausland (2016), Volcano-tectonic earthquakes: A new tool for
362 estimating intrusive volumes and forecasting eruptions, *Journal of Volcanology and*
363 *Geothermal Research*, 309, pp.139-155.
- 364 Wiemer, S. (2001), A software package to analyze seismicity: ZMAP, *Seismological*
365 *Research Letters*, 72(3), pp.373-382.
- 366 Zhang, M. and L. Wen, (2015), Earthquake characteristics before eruptions of Japan's Ontake
367 volcano in 2007 and 2014, *Geophysical Research Letters*, 42(17), pp.6982-6988.

368 **Figure 1.** VT swarm before the 2017 Mount Agung eruption. **(a)** Spatial distribution of
369 epicenters (colored circles) from 1 August to 1 December 2017. Circles are scaled to
370 magnitude. Inverted triangles are BMKG broadband seismic stations. **(b)** Magnitude
371 distribution. Blue solid lines are the cumulative number of earthquakes. **(c)** Spatiotemporal
372 N-S distribution. **(d)** Histogram of frequency-magnitude distribution.

373

374 **Figure 2.** The topography around Mount Agung and relocated epicenters of VT swarm (red
375 circles). Squares are TMKS, PSAG (seismic) and REND (GNSS) station. Stars are $M > 4$
376 events. Also shown three-component seismograms of station SRBI and DNP for the 26
377 September 2017 M4.2 event.

378

379 **Figure 3.** Relocated hypocenters. **(a)** Along the S-N profile. **(b)** Along the SW-NE profile.
380 **(c)** Along the W-E profile. **(d)** Along the NW-SE profile. Orange solid rectangles represent
381 dike inferred by Albino *et al.* (2019).

382

383 **Figure 4.** MFT detection. Example of waveform comparison between a detected event
384 (magnitude 3.1; gray traces) and its detecting template event (magnitude 3.6; red traces). The
385 mean correlation coefficient between all of these waveforms is 0.857. The black arrow shows
386 the origin time of the detected event. The amplitudes were normalized by the maximum value
387 at each window at each component/station. The station name, component/channel, and
388 distance (km) are shown at the beginning of each gray trace. Station locations are plotted in
389 the inset figure.

390

391 **Figure 5.** Swarm seismicity detected by MFT. **(a)** Spatiotemporal evolution of VT
392 earthquakes (circles; colored according to the depth of the hypocenters). Gray triangles are
393 templates. Black stars are $M > 4.1$ events. L2, L3, and L4 correspond to the different alert
394 levels provided by the PVMBG during the crisis. LF=Low Frequency events. The first and
395 second green lines denote the time mark of 22 September and 20 October, respectively (see
396 text). The third green line denotes the time mark when a magnitude 4.9 occurred. The blue
397 dashed line indicates a time mark when the tremor firstly took place. The first and second red
398 lines indicate time when the first phreatomagmatic eruption and the onset of larger
399 explosions, respectively. Blue solid line shows the number of earthquakes per day based on
400 MFT detection. **(b)** Depth-time evolution of VT earthquakes. Solid lines show the corrected
401 InSAR time series detecting displacement anomalies at point 'A' (see Fig. 2) provided by
402 Albino *et al.* (2020). **(c)** GNSS time-series from station REND (N) and 12 hours RSAM from
403 station TMKS (Syahbana *et al.*, 2019). **(d)** Magnitude distribution of MFT-based VT
404 seismicity colored by different detection thresholds. Red circles are templates. The solid blue
405 line corresponds to the cumulative number of events.

Figure 1. VT swarm before the 2017 Mount Agung eruption. **(a)** Spatial distribution of epicenters (colored circles) from 1 August to 1 December 2017. Circles are scaled to magnitude. Inverted triangles are BMKG broadband seismic stations. **(b)** Magnitude distribution. Blue solid lines are the cumulative number of earthquakes. **(c)** Spatiotemporal N-S distribution. **(d)** Histogram of frequency-magnitude distribution.

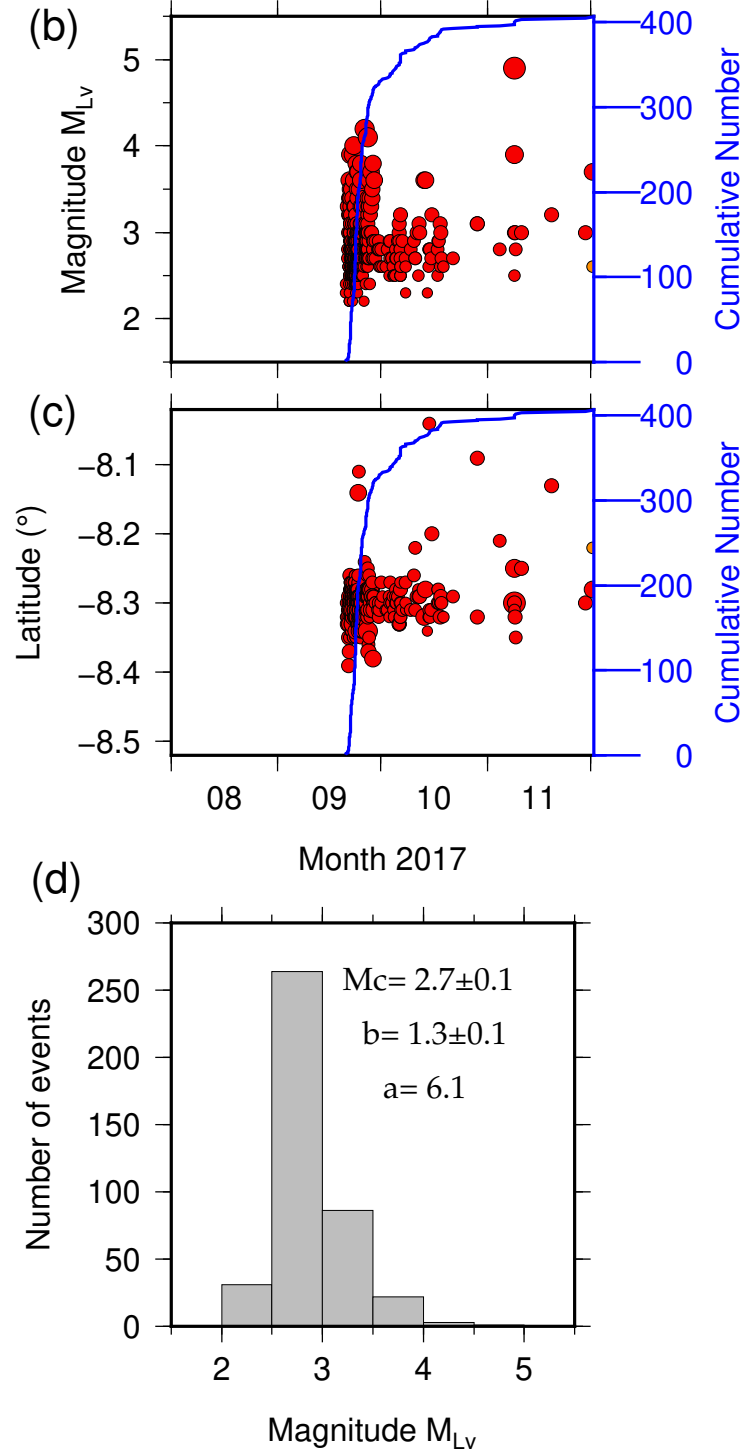
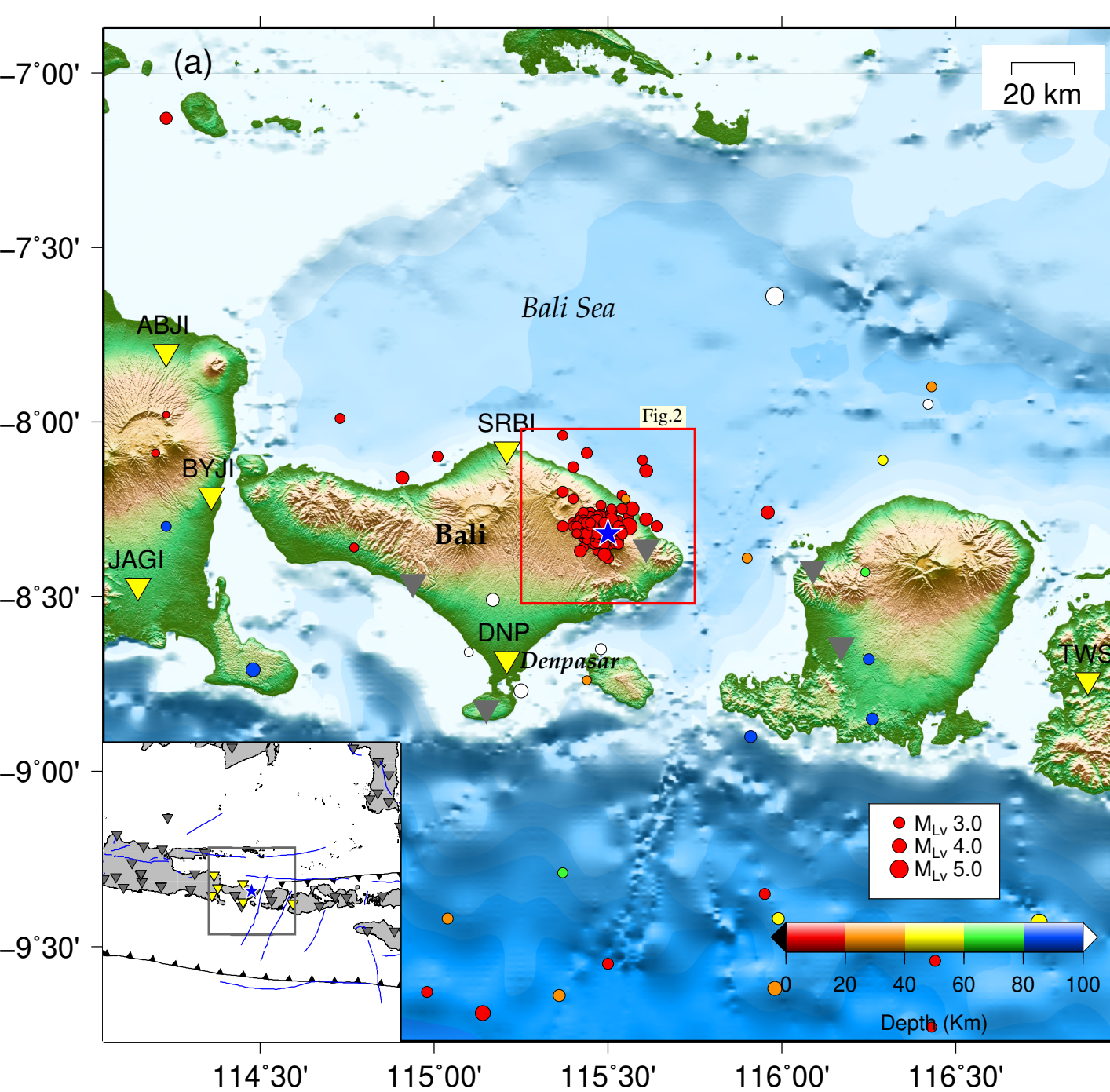


Figure 2. The topography around Mount Agung and relocated epicenters of VT swarm (red circles). Squares are TMKS, PSAG (seismic) and REND (GNSS) station. Stars are $M > 4$ events. Also shown three-component seismograms of station SRBI and DNP for the 26 September 2017 M4.2 event.

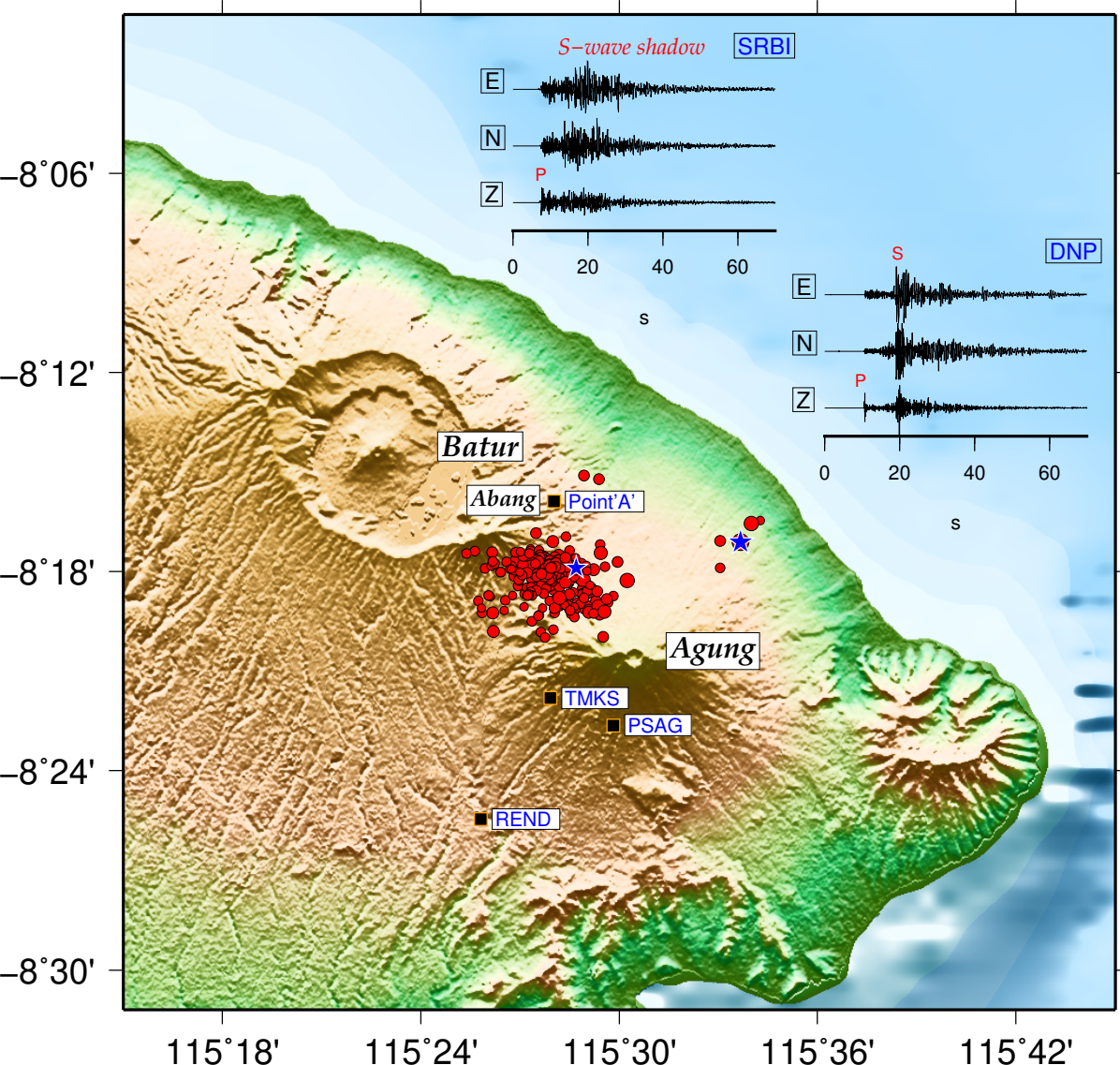


Figure 3. Relocated hypocenters. **(a)** Along the S-N profile. **(b)** Along the SW-NE profile. **(c)** Along the W-E profile. **(d)** Along the NW-SE profile. Orange solid rectangles represent dike inferred by Albino *et al.* (2019).

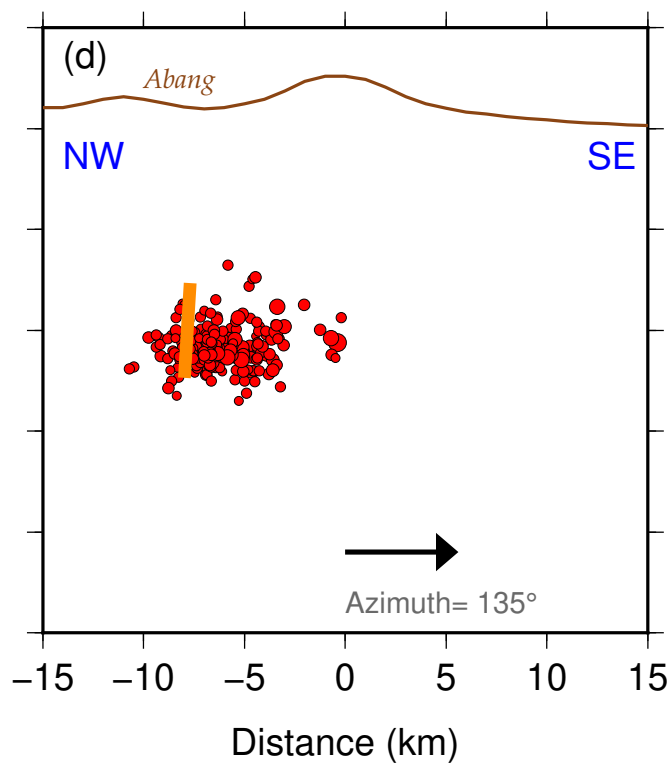
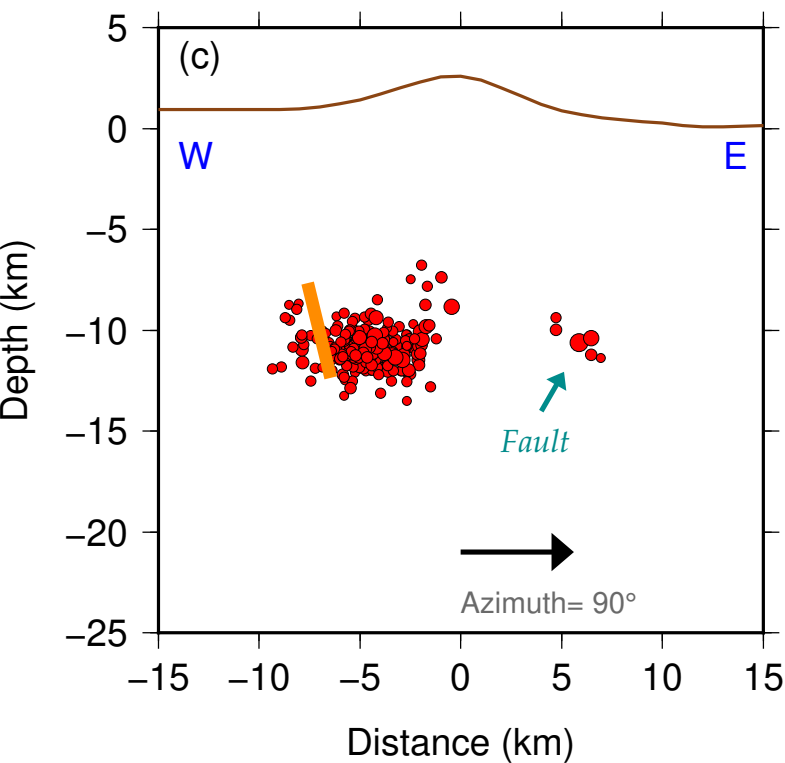
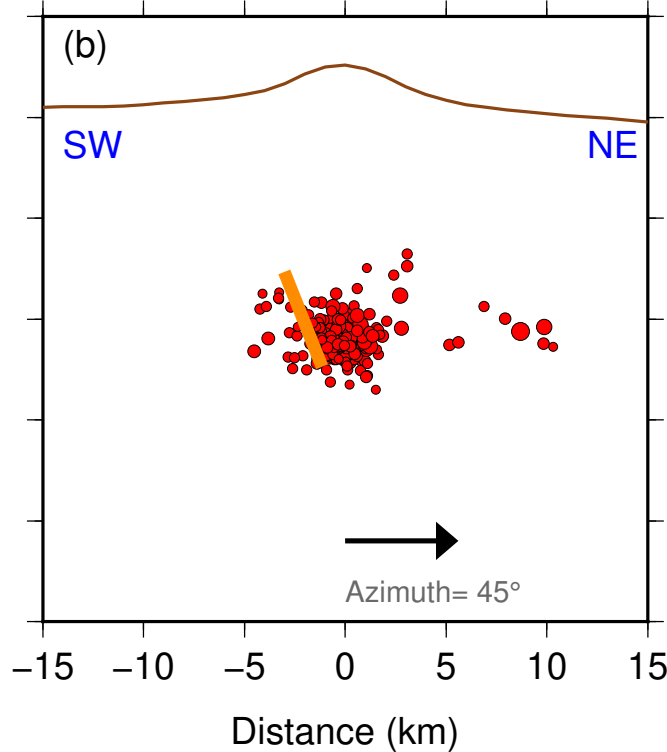
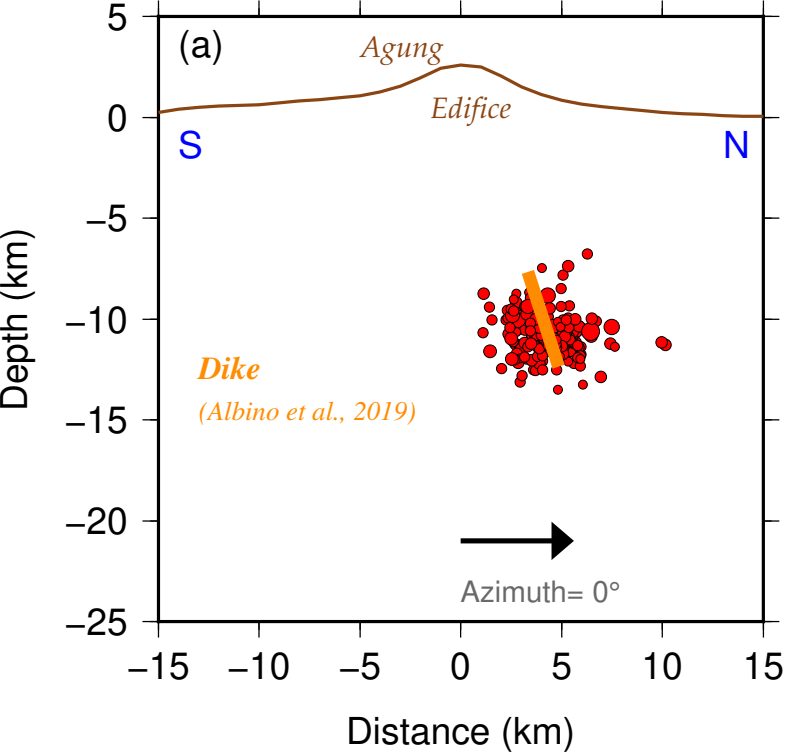
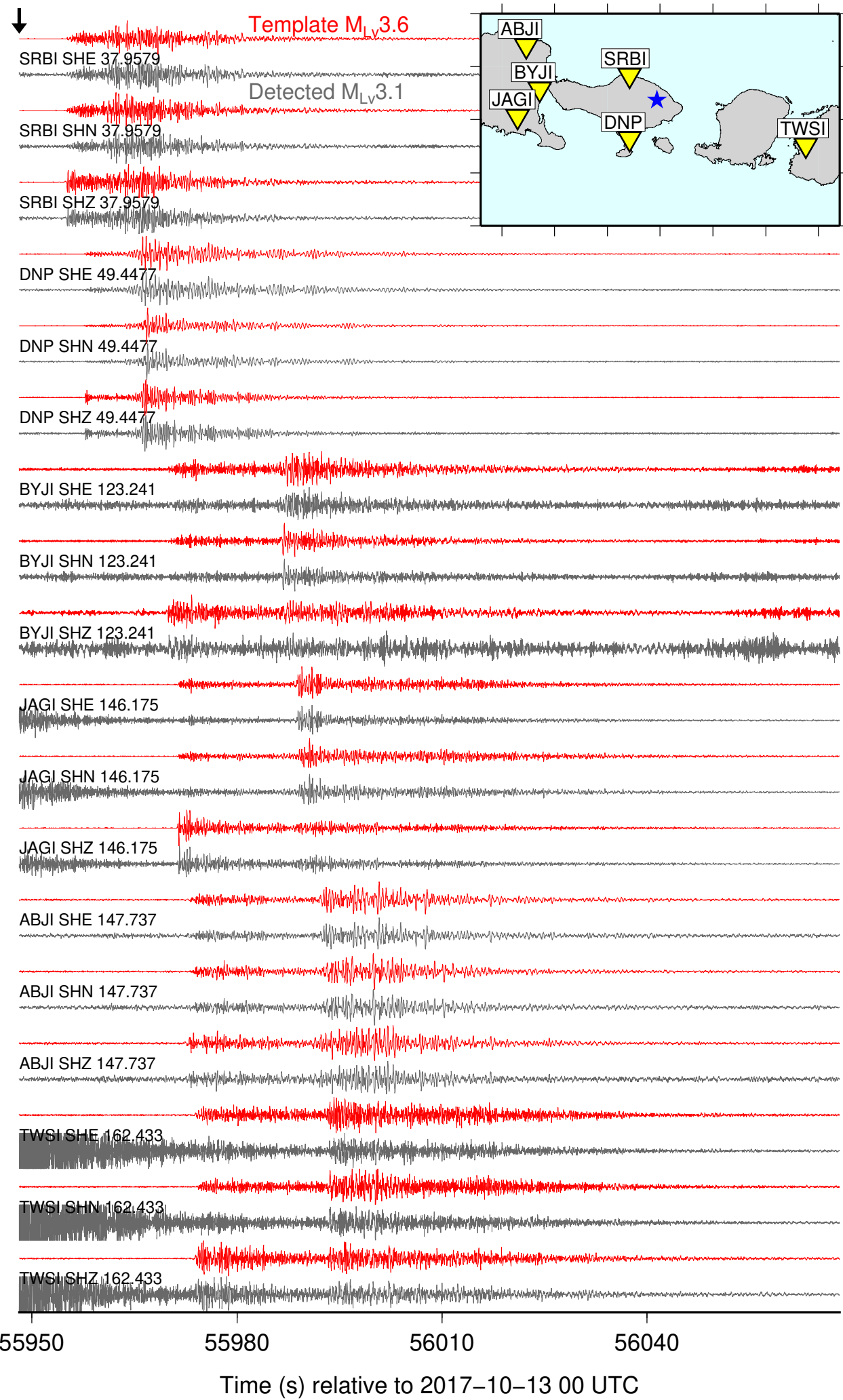
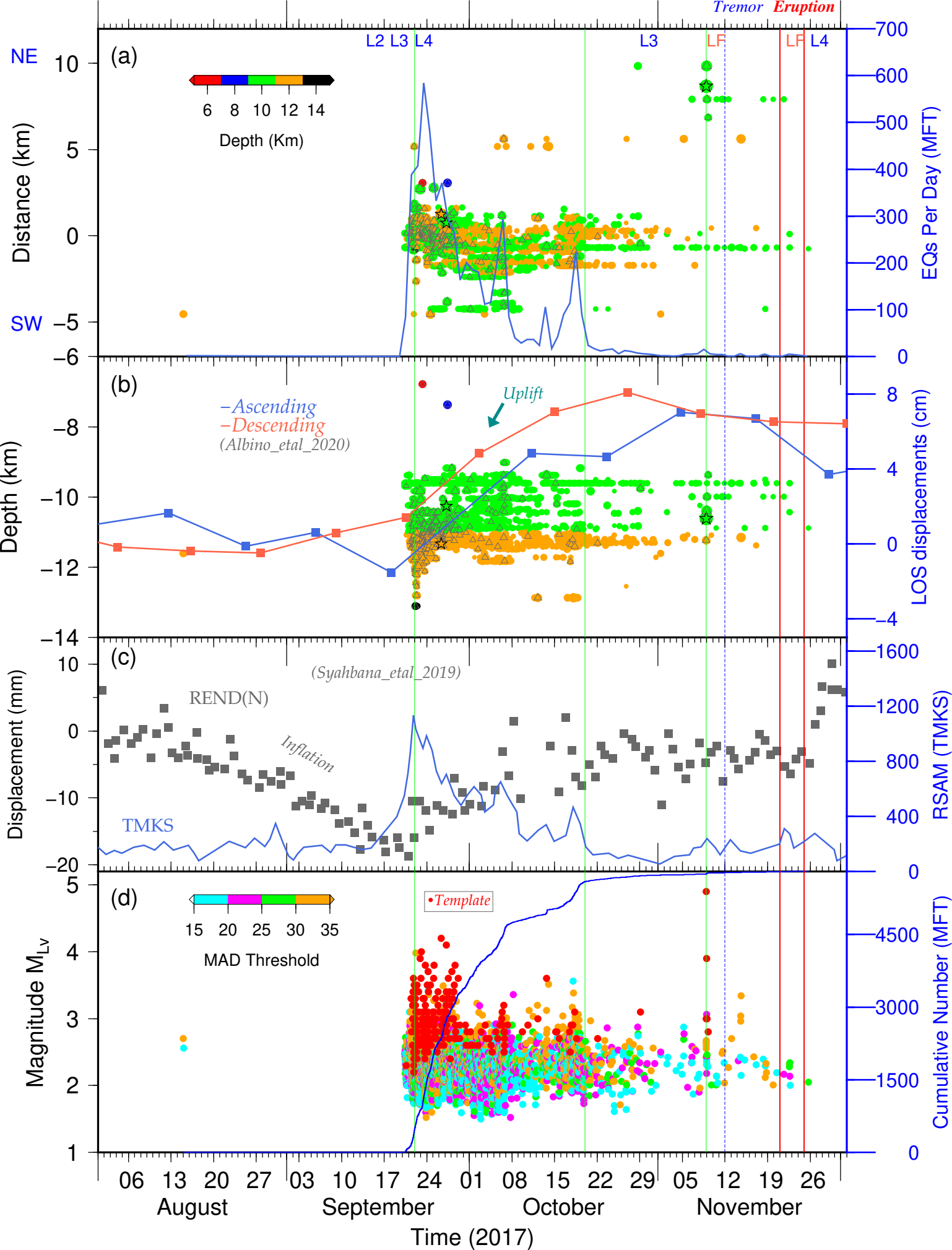


Figure 4. MFT detection. Example of waveform comparison between a detected event (magnitude 3.1; gray traces) and its detecting template event (magnitude 3.6; red traces). The mean correlation coefficient between all of these waveforms is 0.857. The black arrow shows the origin time of the detected event. The amplitudes were normalized by the maximum value at each window at each component/station. The station name, component/channel, and distance (km) are shown at the beginning of each gray trace. Station locations are plotted in the inset figure.



1 **Figure 5.** Swarm seismicity detected by MFT. **(a)** Spatiotemporal evolution of VT
2 earthquakes (circles; colored according to the depth of the hypocenters). Gray triangles are
3 templates. Black stars are $M > 4.1$ events. L2, L3, and L4 correspond to the different alert
4 levels provided by the PVMBG during the crisis. LF=Low Frequency events. The first and
5 second green lines denote the time mark of 22 September and 20 October, respectively (see
6 text). The third green line denotes the time mark when a magnitude 4.9 occurred. The blue
7 dashed line indicates a time mark when the tremor firstly took place. The first and second red
8 lines indicate time when the first phreatomagmatic eruption and the onset of larger
9 explosions, respectively. Blue solid line shows the number of earthquakes per day based on
10 MFT detection. **(b)** Depth-time evolution of VT earthquakes. Solid lines show the corrected
11 InSAR time series detecting displacement anomalies at point 'A' (see Fig. 2) provided by
12 Albino *et al.* (2020). **(c)** GNSS time-series from station REND (N) and 12 hours RSAM from
13 station TMKS (Syahbana *et al.*, 2019). **(d)** Magnitude distribution of MFT-based VT
14 seismicity colored by different detection thresholds. Red circles are templates. The solid blue
15 line corresponds to the cumulative number of events.

16



Supporting Information for

Seismic swarm preceding the 2017 Mount Agung eruption in Bali (Indonesia) enhanced by the matched filter approach

Dimas Sianipar^{1,2}, Emi Ulfiana^{1,3}, Renhard Sipayung^{1,4}

¹Badan Meteorologi, Klimatologi, dan Geofisika (BMKG), Jakarta 10720, Indonesia

²Sekolah Tinggi Meteorologi, Klimatologi, dan Geofisika (STMKG), Tangerang Selatan, Banten, 15221, Indonesia

³BMKG Stasiun Geofisika Sanglah, Denpasar, Bali, Indonesia

⁴BMKG Stasiun Geofisika Banjarnegara, Jawa Tengah, Indonesia

Contents of this file

Text S1 Hypocenter relocation

Text S2 Magnitude homogenization

Text S3 Calculation of M_c and b-value

Additional Supporting Information (Files uploaded separately)

Captions for Figure S1 to S12

Captions for Table S1 to S2

Text S1. [Hypocenter Relocation]

We selected seismic data from six BMKG regional broadband three-component stations (i.e., 18 channels) with a distance less than 170 km from the summit and with good azimuthal coverage, i.e., station SRBI (~37 km), DNP (~49 km), BYJI (~123 km), JAGI (~146 km), ABJI (~147 km), and TWSI (~162 km). We were lacking a local broadband station close to the summit of Mount Agung (Fig. 2, S8); however, two of our stations located within <50 km distance from Mount Agung.

We visually picked the arrival times of the P- and S-waves of 407 VT earthquakes between 1 August and 1 December 2017. In addition to the catalog of arrival times, we also used differential arrival times obtained by the waveform cross-correlation method. The time window for cross-correlation is within a 2s; 0.5 s before and 1.5 s after the hand-picked P/S arrival times for seismograms bandpass filtered between 1 and 15 Hz. We relocated the events using double-difference method applied in HypoDD code (Waldhauser and Ellsworth, 2000). We used the global 1D velocity model (IASP91; Kennett and Engdahl, 1991) because the local velocity structure of Mount Agung has not been previously investigated. The maximum hypocentral separation is 5 km, and the maximum number of neighbors per event is 20. The minimum four links are chosen for clustering. Fig. S1 and S2 show the position of earthquakes before relocation, and Fig. 1 and 2 show the refined positions after the relocation. The relocated hypocenters mostly located at 9 to 13 km of depths (Fig. 3).

It is noteworthy that Pusat Vulkanologi dan Mitigasi Bencana Geologi (PVMBG) operated two short-period seismic stations during the 2017 unrest located on the S and SW flanks of Mount Agung, ~4 and 5 km from the summit, i.e., station TMKS and PSAG (Fig. 2). Besides, station REND is one of five continuous GNSS stations that used to monitor the deformation of Mount Agung. This station located ~12 km S-SW of the volcano's summit (Fig. 2).

Text S2. [Magnitude Homogenization]

All of the preferred magnitude used in the BMKG catalog for earthquakes analyzed in this study was in the type of M_{LV} (local magnitude measured on the vertical component), except for the 8 November 2017 21:54 UTC event that use moment magnitude ($M_w=4.9$). The local magnitude (M_{LV}) for this event is 5.2.

Text S3. [Calculation of M_c and b-value]

We calculated the magnitude of completeness (M_c) using the maximum curvature (MAXC) technique applied in the ZMAP Matlab code (Wiemer, 2001). This method worked quickly by defining the point of the maximum curvature as the magnitude of completeness by computing the maximum value of the first derivative of the frequency-magnitude curve. The uncertainty was determined by a bootstrap approach. The comparison of FMD before and after performing MFT detection is provided in Fig. S3. The b and a values and their respective uncertainties are computed using a maximum-likelihood assessment (Shi and Bolt, 1982).

References:

Kennett, B. L. N., & Engdahl, E. R. (1991). Traveltimes for global earthquake location and phase identification. *Geophysical Journal International*, 105(2), 429-465.

Shi, Y., & Bolt, B. A. (1982). The standard error of the magnitude-frequency b value. *Bulletin of the Seismological Society of America*, 72(5), 1677-1687.

Waldhauser, F., & Ellsworth, W. L. (2000). A double-difference earthquake location algorithm: Method and application to the northern Hayward fault, California. *Bulletin of the Seismological Society of America*, 90(6), 1353-1368.

Wiemer, S. (2001). A software package to analyze seismicity: ZMAP. *Seismological Research Letters*, 72(3), 373-382.

Figure S1. Similar plot with Fig. 2 for un-relocated epicenters.

Figure S2. Similar plot with Fig. 3 for un-relocated hypocenters.

Figure S3. Frequency-magnitude distribution (FMD) for (a) BMKG catalog or before MFT, and (b) MFT catalog.

Figure S4. Record of the 26 September 2017 M4.2 earthquake at station SRBI component vertical. (a) Raw data, (b) band-pass filtered 1-15 Hz, (c) spectrogram.

Figure S5. Similar plot with Fig. S4 for station DNP component vertical.

Figure S6. Record of the 8 November 2017 M4.9 earthquake at station SRBI component vertical. (a) Raw data, (b) band-pass filtered 1-15 Hz, (c) spectrogram.

Figure S7. Similar plot with Fig. S6 for station DNP component vertical.

Figure S8. Similar plot with Fig. 2 but the seismograms are for the 8 November 2017 M4.9.

Figure S9. Similar plot with Fig. 4 for the detection of 2017-09-21 09:07:17 M3.1 event. The black traces are for SNR<5 (not used in MFT).

Figure S10. Three-component seismograms at station SRBI for a newly detected event on 15 August 00:33:02.97 event.

Figure S11. Similar plot with Fig. S10 for 01:44:02.45 event.

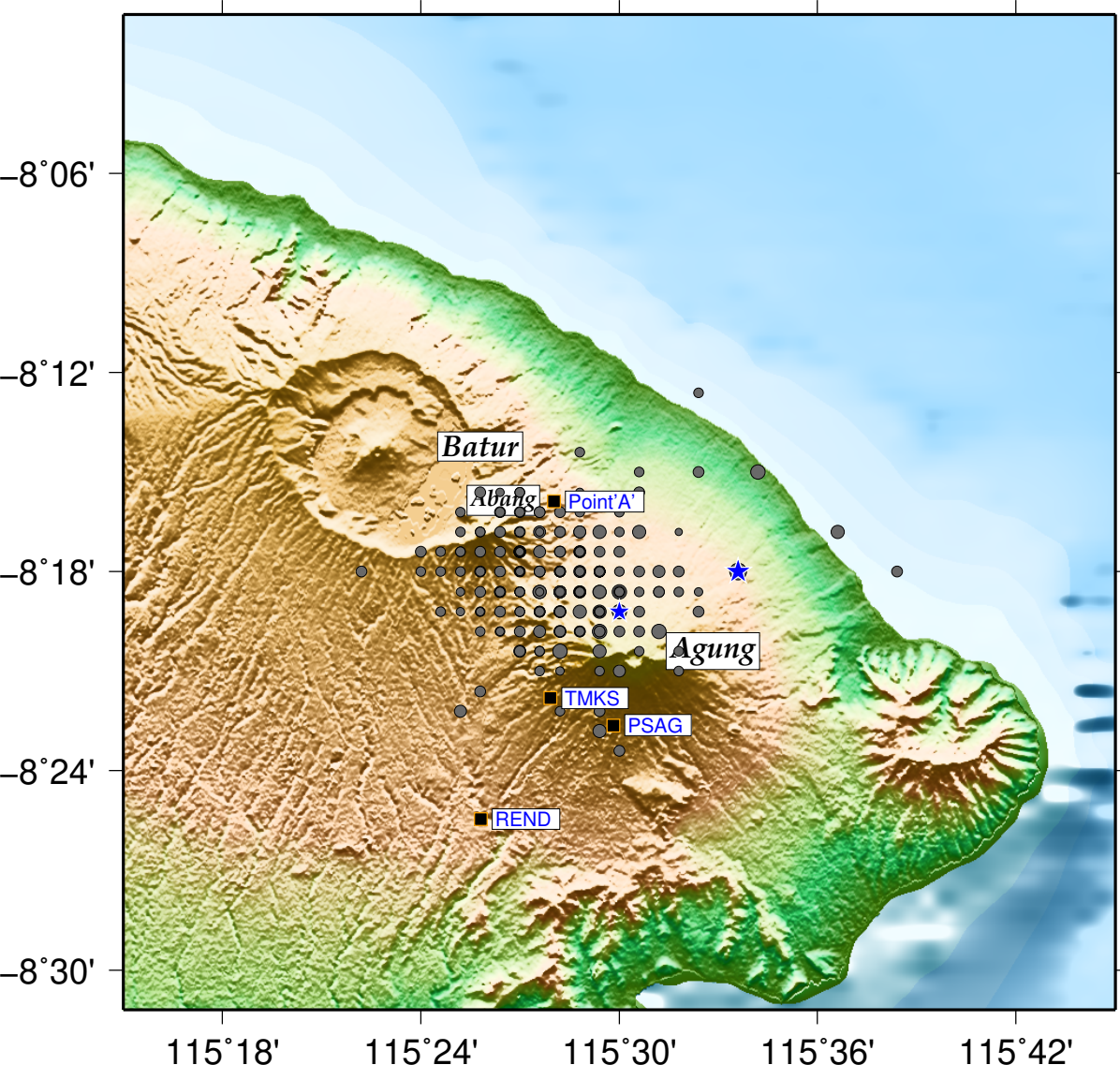
Figure S12. Earthquake statistics using the MFT catalog. (a) Time histogram. (b) Depth histogram. (c) Magnitude histogram. (d) Cumulative seismic moment.

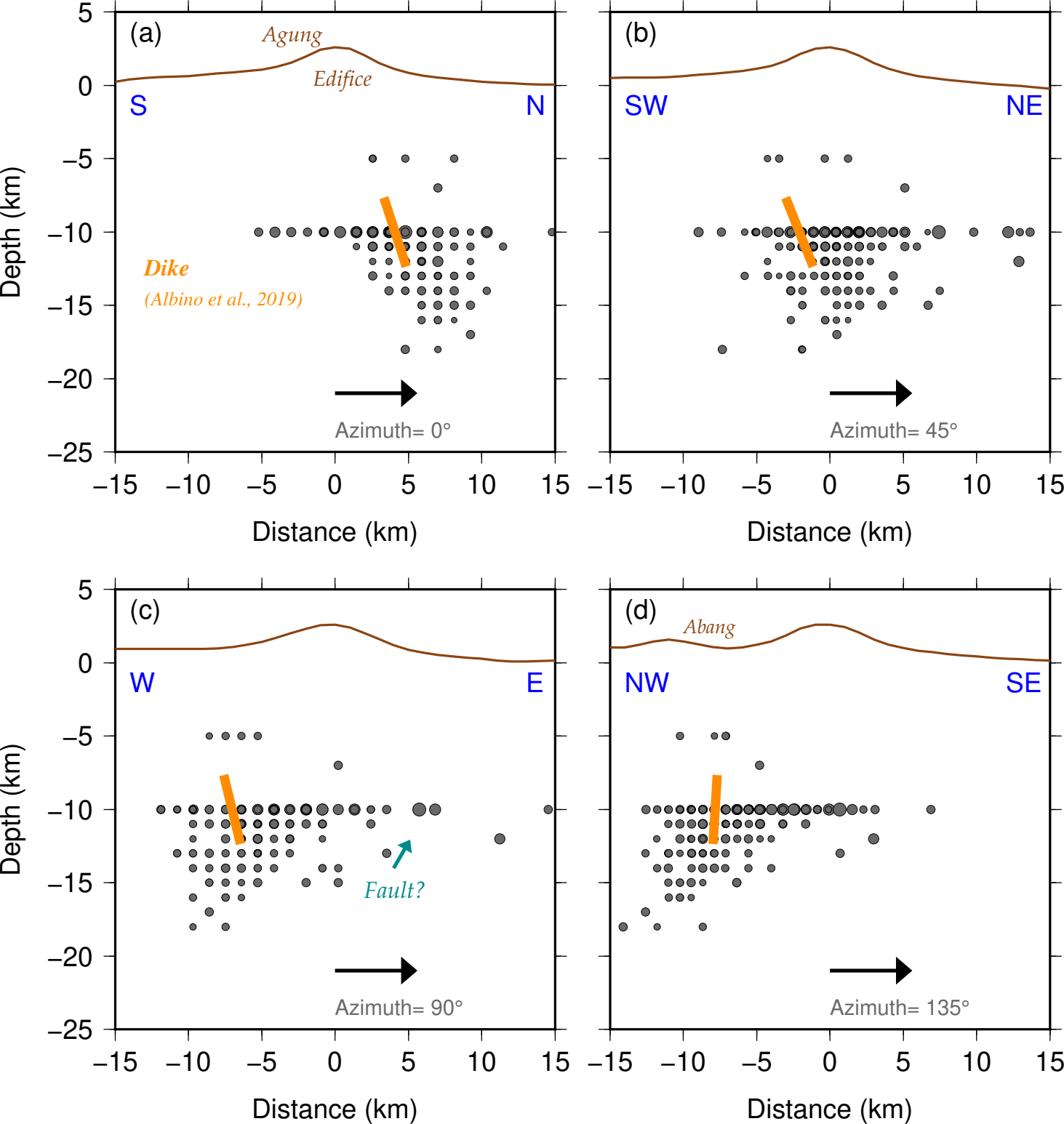
Table S1 List of relocated template candidates (templates library).

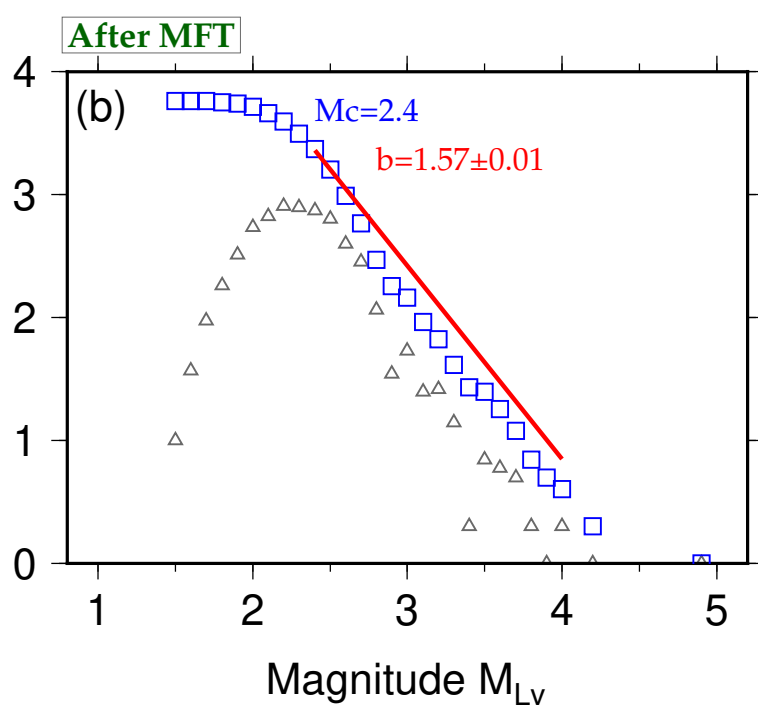
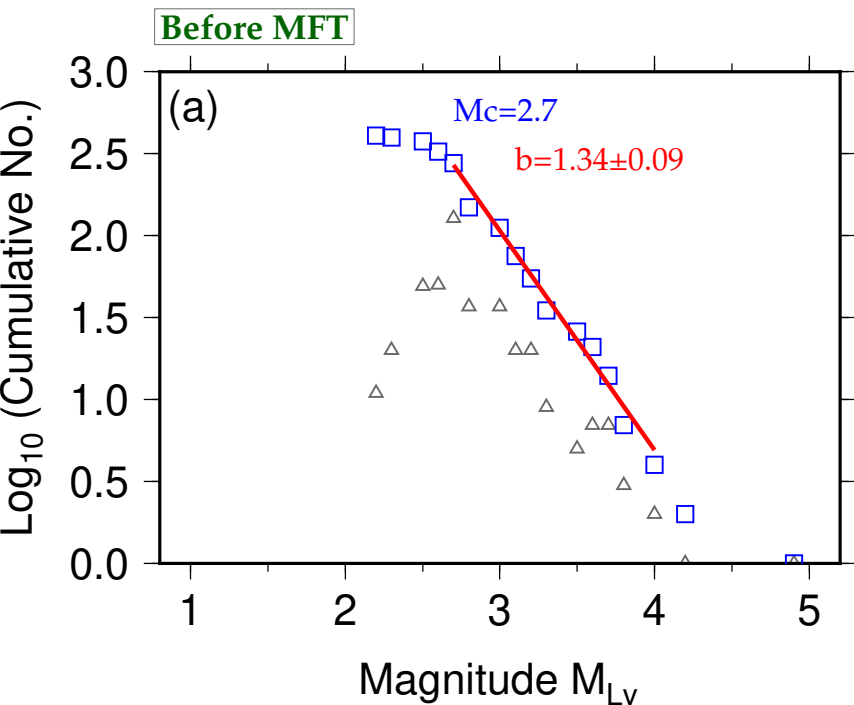
Table S2 Matched filter catalog.

Mean CC= Mean correlation coefficient (Mean CC 1.0= self detection for 257 templates SNR>5).

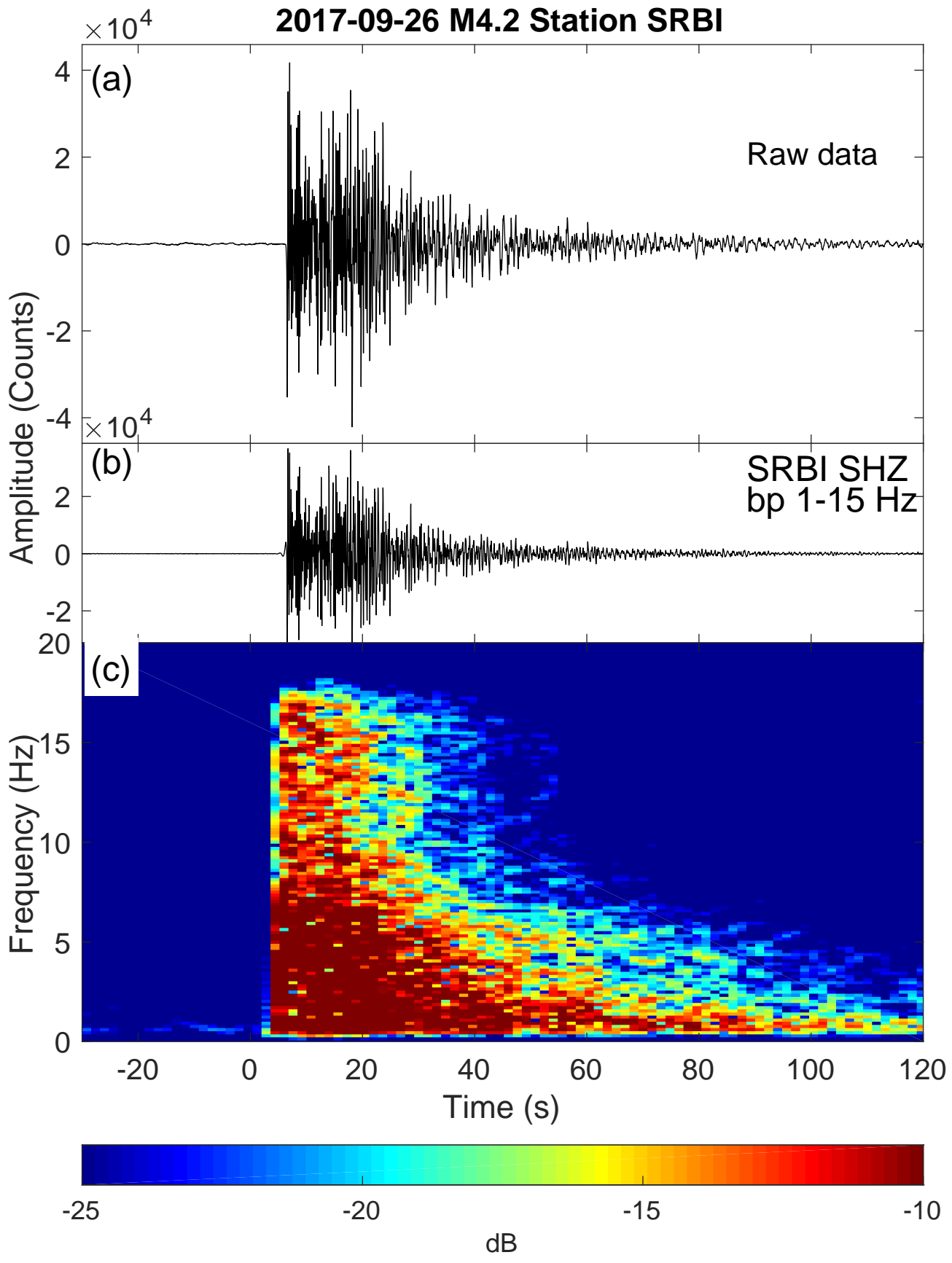
MAD= Median Absolute Deviation.



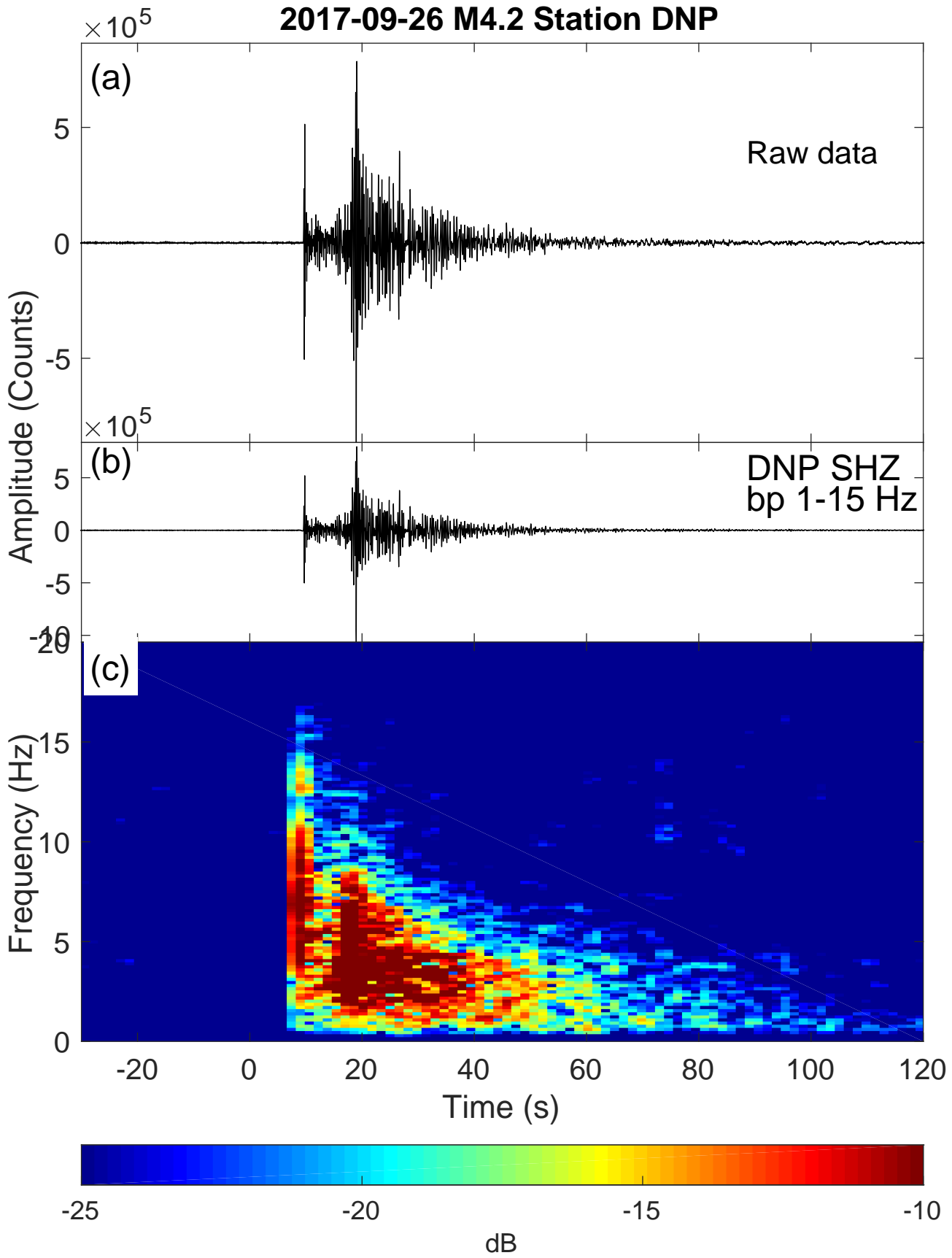




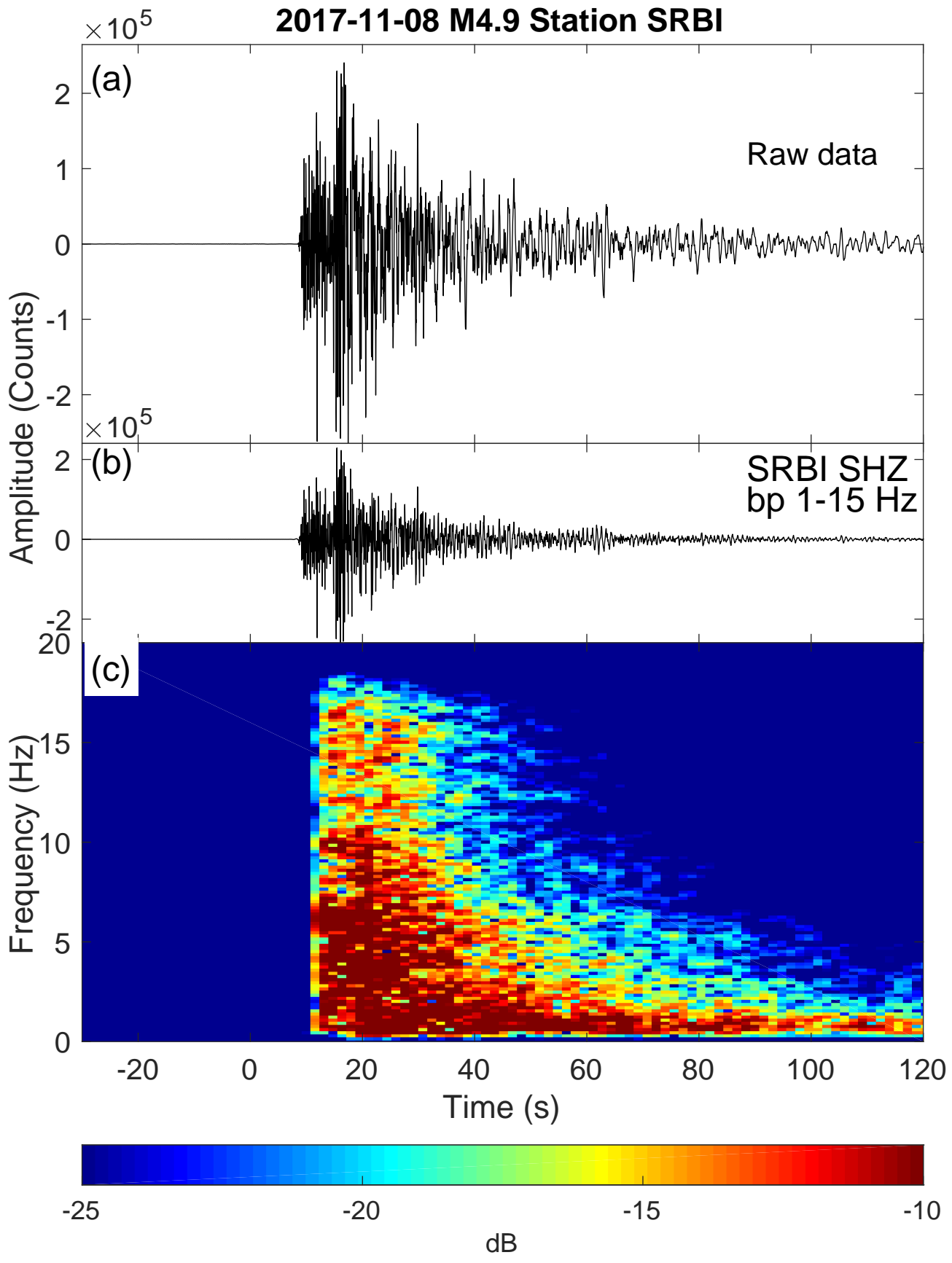
2017-09-26 M4.2 Station SRBI



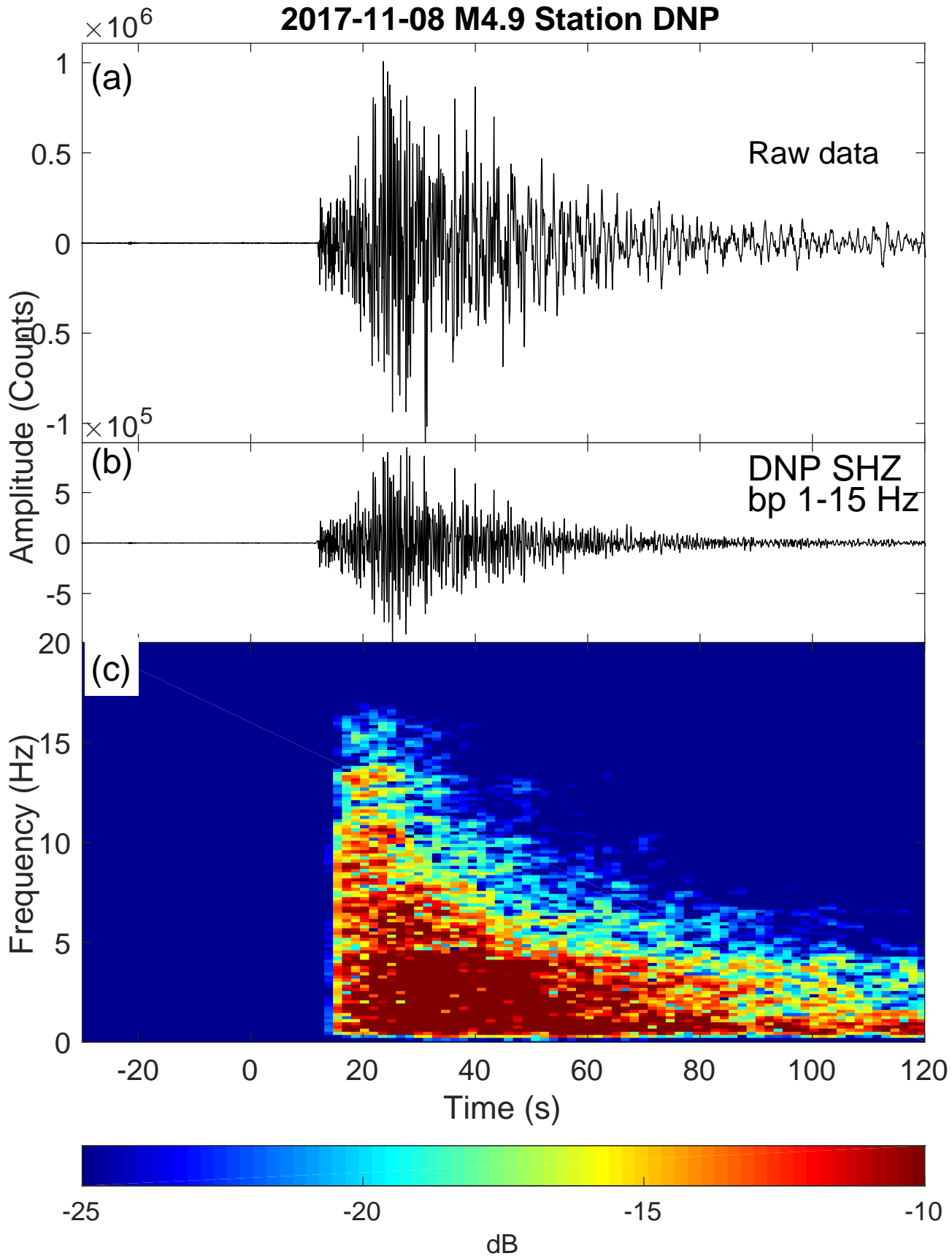
2017-09-26 M4.2 Station DNP

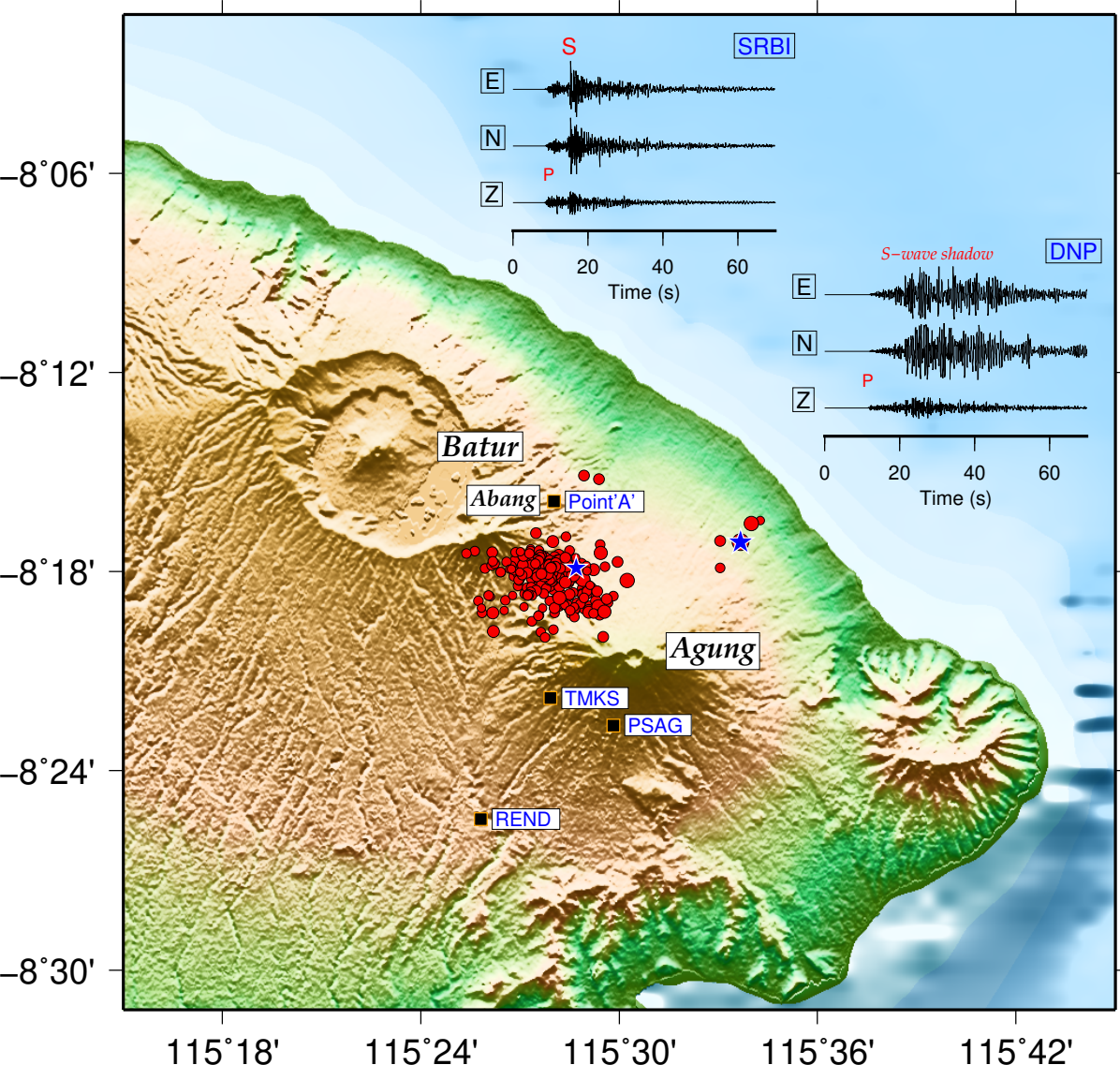


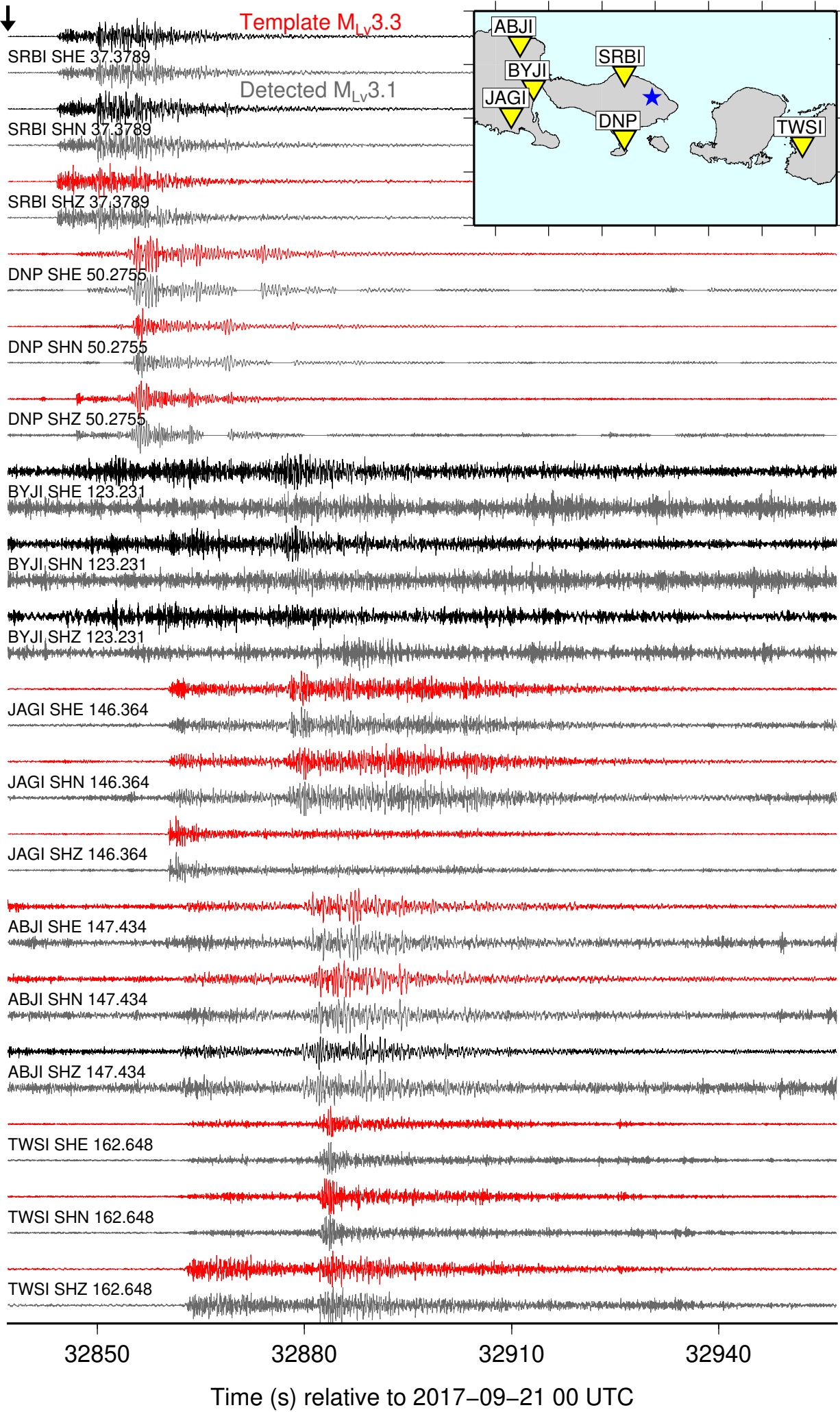
2017-11-08 M4.9 Station SRBI



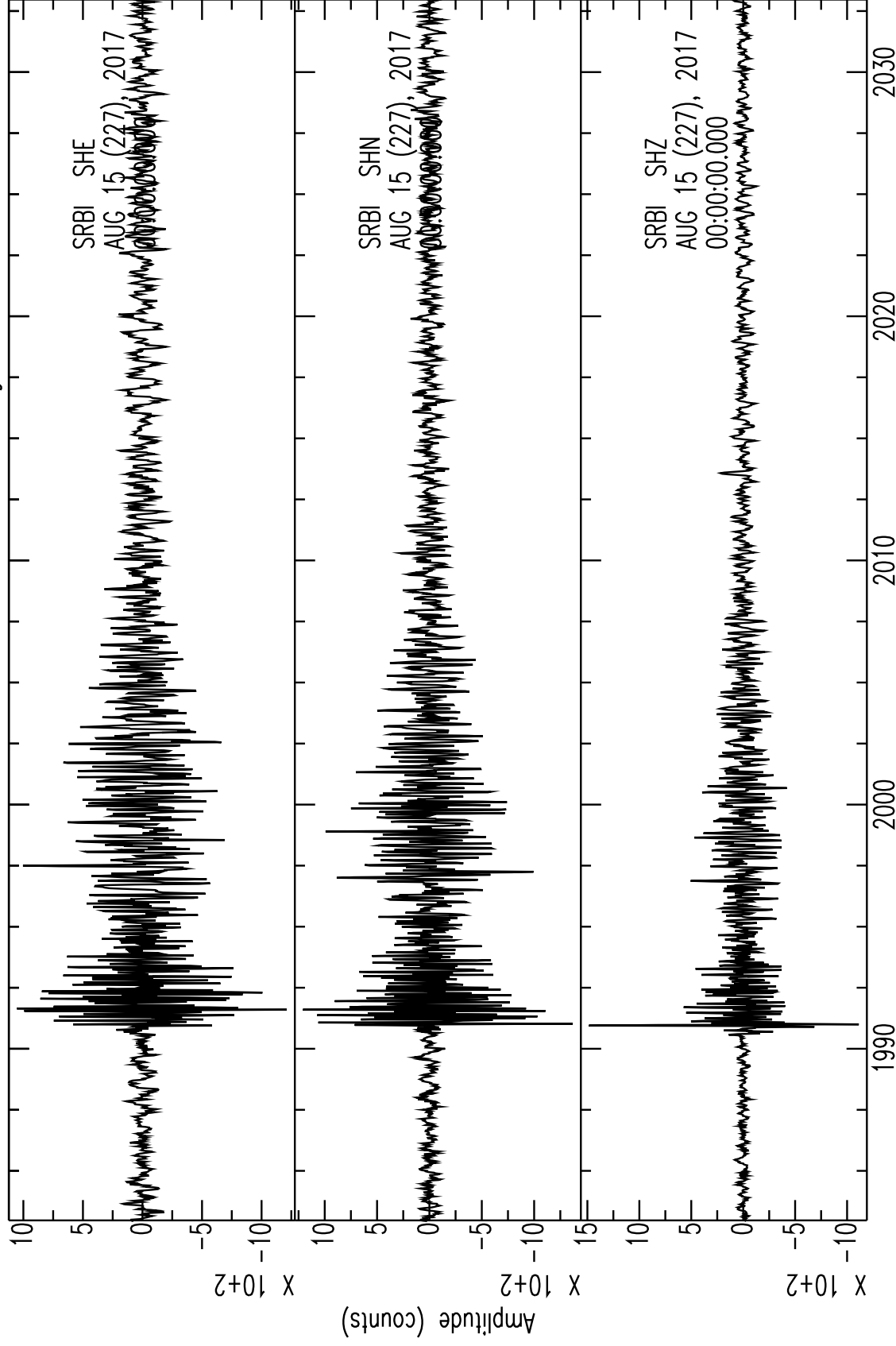
2017-11-08 M4.9 Station DNP



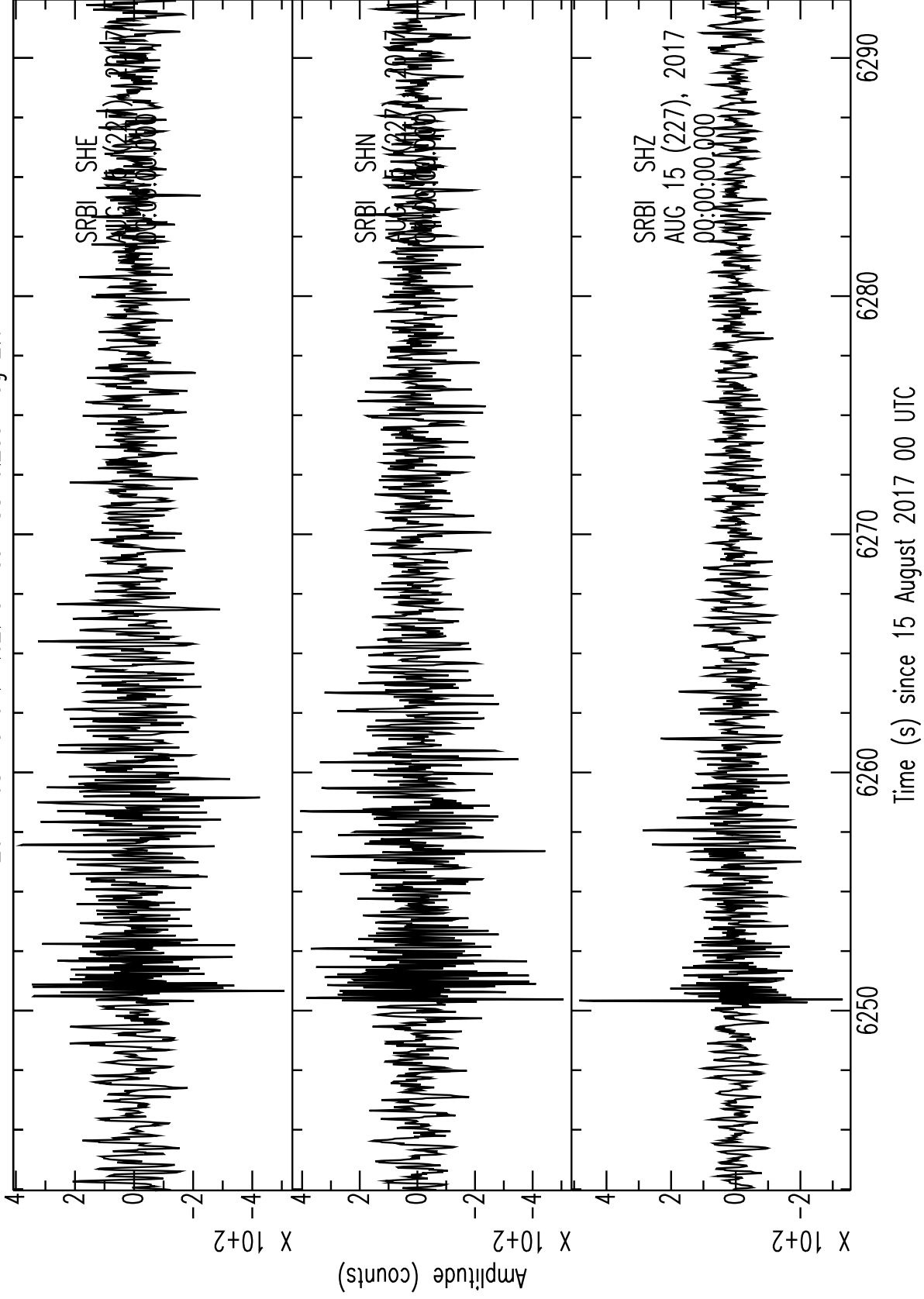


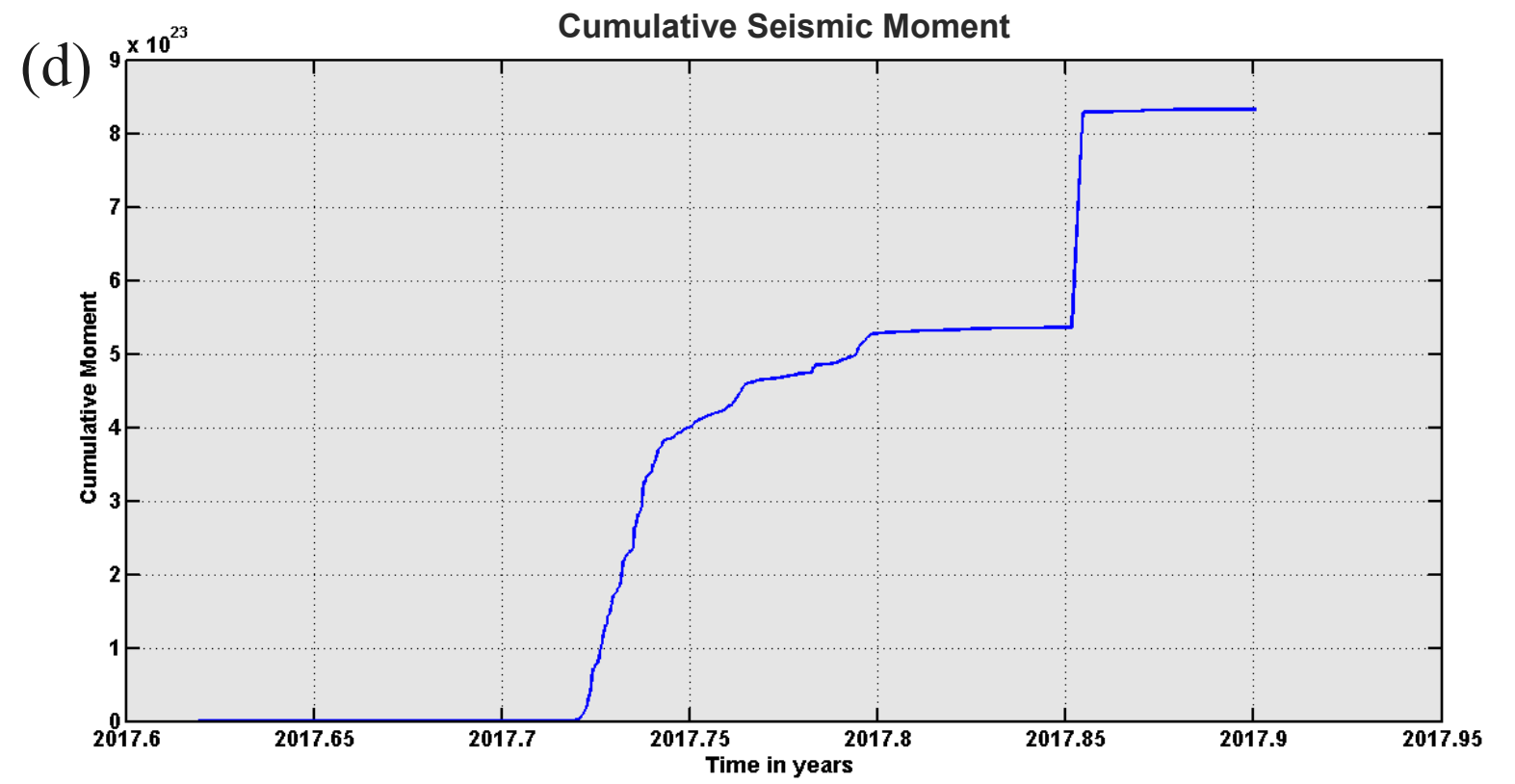
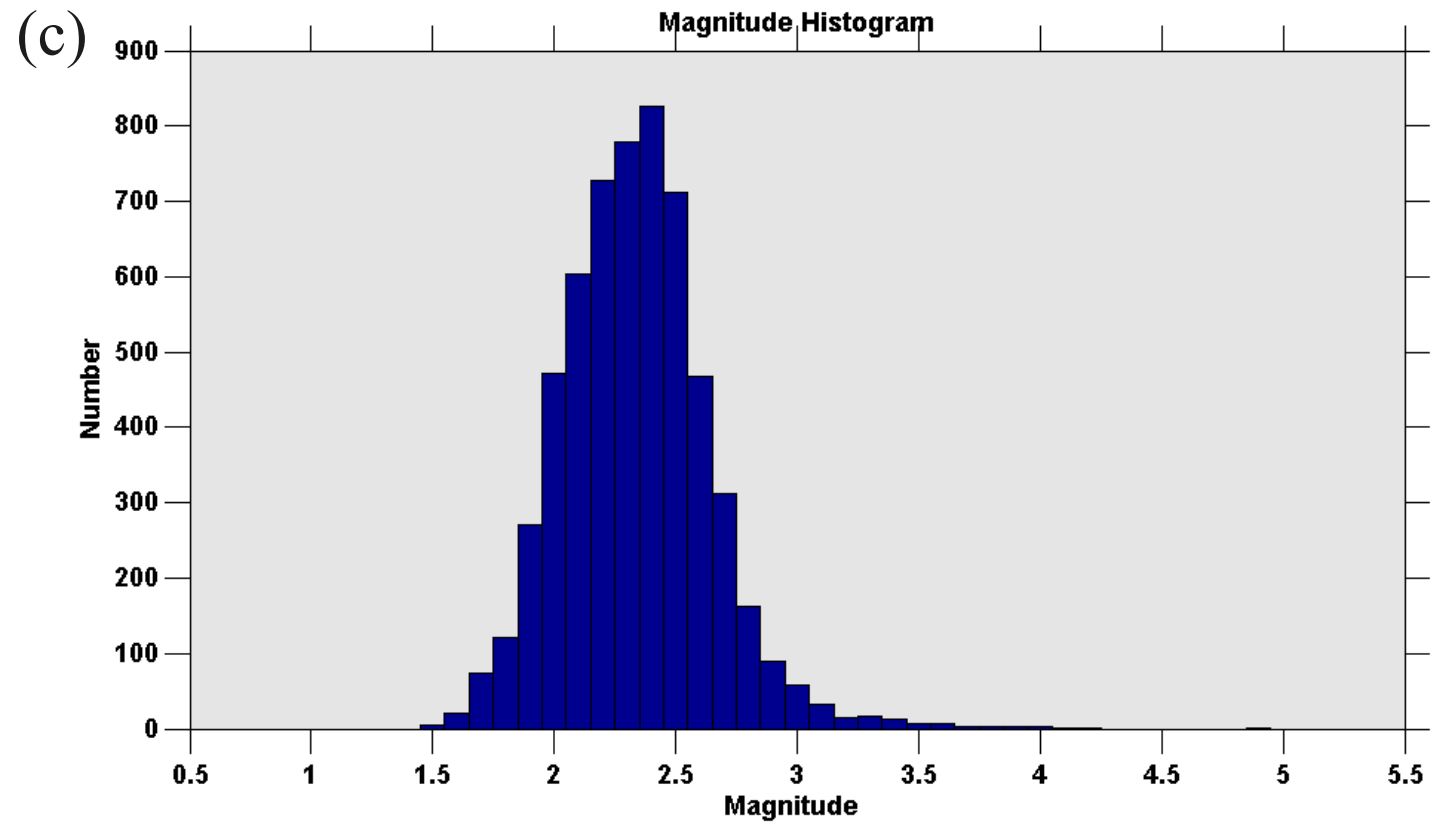
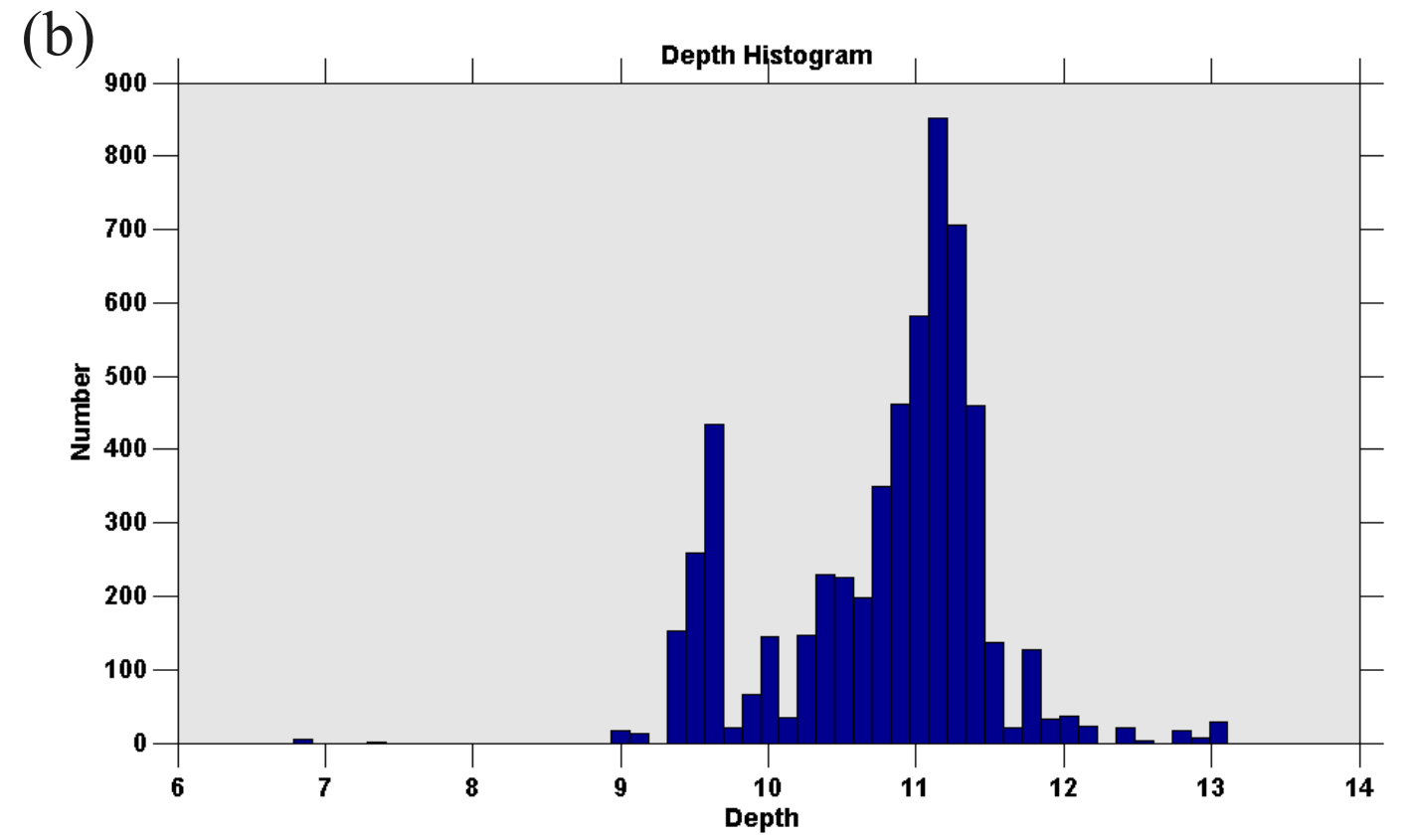
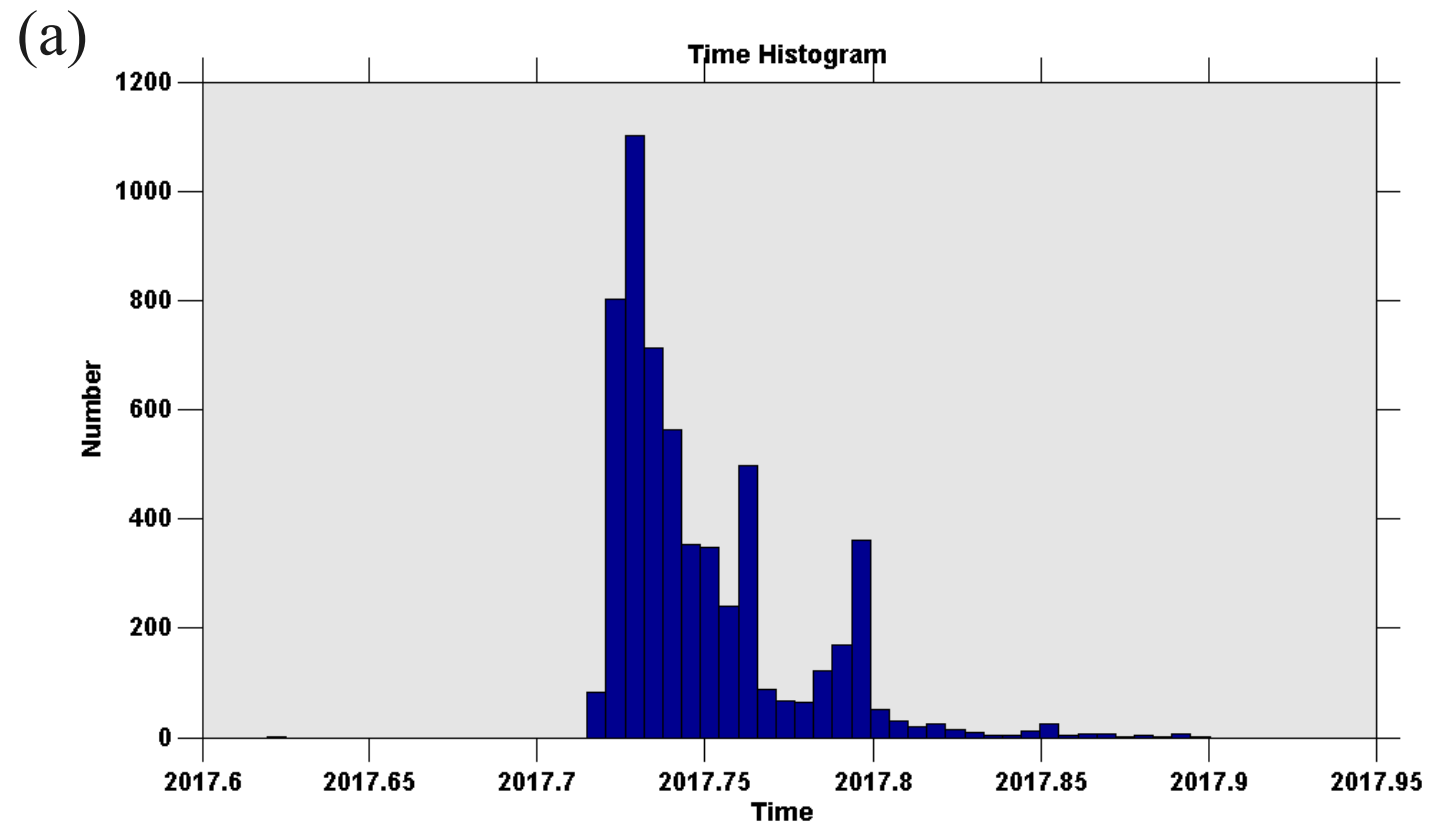


2017-08-15 00:33:02.97 Mean CC=0.477 Mag 2.7



2017-08-15 01:44:02.45 Mean CC=0.253 Mag 2.6





This is a non-peer reviewed pre-print that has been submitted for publication